NACA L-175

ARR No. L5C01

NATIONAL ADVISORY COMMITTEE FOR AERONAUTICS

WARTIME REPORT

ORIGINALLY ISSUED
March 1945 as
Advance Restricted Report L5C01

WIND-TUNNEL INVESTIGATION OF CONTROL-SURFACE CHARACTERISTICS XXI - MEDIUM AND LARGE AERODYNAMIC BALANCES OF TWO NOSE SHAPES AND A PLAIN OVERHANG USED WITH A 0.40-AIRFOIL-CHORD FLAP ON AN NACA 0009 AIRFOIL

By John M. Riebe and Oleta Church

Langley Memorial Aeronautical Laboratory
Langley Field, Va.

UNIVERSITY OF FLORIDA
DOCUMENTS DEPARTMENT
120 MARSTON SCIENCE LIBRARY
P.O. BOX 117011
GAINESVILLE, FL 32611-7011 USA

WASHINGTON

NACA WARTIME REPORTS are reprints of papers originally issued to provide rapid distribution of advance research results to an authorized group requiring them for the war effort. They were previously held under a security status but are now unclassified. Some of these reports were not technically edited. All have been reproduced without change in order to expedite general distribution.

Digitized by the Internet Archive
in 2011 with funding from
University of Florida, George A. Smathers Libraries with support from LYRASIS and the Sloan Foundation

http://www.archive.org/details/windtunnelst00l

3807479

NACA ARR No. L5C01 RESTRICTED

NATIONAL ADVISORY COMMITTEE FOR AERONAUTICS

ADVANCE RESTRICTED REPORT

WIND-TUNNEL INVESTIGATION OF CONTROL-SURFACE CHARACTERISTICS XXI - MEDIUM AND LARGE AERODYNAMIC BALANCES OF TWO NOSE SHAPES AND A PLAIN OVERHANG USED WITH A 0.40-AIRFOIL-CHORD FLAP ON AN NACA 0009 AIRFOIL

By John M. Riebe and Oleta Church

SUMMARY

Wind-tunnel tests have been made to investigate the characteristics of an NACA 0009 airfoil with a 40-percent-chord flap having medium and large aerodynamic balances of elliptical and blunt nose shapes and having a plain overhang. The results are presented as aerodynamic section characteristics for several flap deflections with the gap at the flap nose sealed and unsealed. Tests were also made to determine the effectiveness of a tab, which was 20 percent of the flap chord, on the plain sealed flap and on the 35-percent-flap-chord elliptical-overhang flap with gap sealed. The pressure difference across the flap-nose seal was also determined for the plain sealed flap.

The results indicate that the slope of the lift-coefficient curve was approximately the same for all sealed-gap conditions, except for the flap with a 50-percent-flap-chord elliptical overhang for which the slope was about 3 percent larger than the average. A 4-percent reduction of slope occurred as a result of unsealing the gap at the flap nose on the plain flap; whereas a 13- to 17-percent reduction occurred as a result of unsealing the gap at the flap nose on the flap with aerodynamic balance. The change in lift with flap deflection was found to increase as a result of sealing the gap at the flap nose and of changing the nose shape from elliptical to blunt.

The effect of unsealing the gap (except for the plain flap), increasing the balance length, and changing the nose shape from elliptical to blunt was to make the rate of change of flap hinge moment with flap deflection (at small flap deflections) and with angle of attack more positive. Some overbalance was found on the 50-percent-flap-chord overhangs.

When the lift was varied by changing the angle of attack at zero flap deflection, the center of lift was at the 24-percent-chord station for all overhangs tested with gap sealed. The center of lift due to angle of attack and that due to flap deflection generally moved rearward as the gap was unsealed.

INTRODUCTION

The NACA is conducting an extensive investigation to provide experimental data for design purposes and to determine the section characteristics of various types of flap arrangement suitable for use as control surfaces. The investigation is being made in the Langley 4- by 6-foot vertical tunnel and has included tests in which flap profile, trailing-edge angle, gap size, flap nose shape, and balance-chord length have been varied. Most of these tests have been made, however, of a 30-percent-chord flap. In the present report, the investigation is extended to determine the effects of flap nose shape and balance-chord length on an airfoil having a 40-percent-chord flap. Data on the pressure across the seal of the plain-flap nose and a method of applying these pressure data in the design of internal balances are presented. Tab data are presented for a flap with a plain overhang and with aerodynamic balance.

SYMBOLS

The coefficients and the symbols used are defined as follows:

c_l airfoil section lift coefficient $\left(\frac{l}{qc}\right)$

c_{d_o} airfoil section profile-drag coefficient $\left(\frac{d_o}{qc}\right)$

Δc_{d_o} increment of section profile-drag coefficient due to flap deflection

c_m airfoil section pitching-moment coefficient $\left(\frac{m}{qc^2}\right)$

c_{h_f} flap section hinge-moment coefficient $\left(\frac{h_f}{qc_f^2}\right)$

c_{h_t} tab section hinge-moment coefficient $\left(\frac{h_t}{qc_t^2}\right)$

p_R resultant pressure coefficient $\left(\frac{p_L - p_U}{q}\right)$

where

l airfoil section lift

d_o airfoil section profile drag

m airfoil section pitching moment about quarter-chord point of airfoil (positive moment moves nose of airfoil up)

h_f flap section hinge moment about flap hinge axis (positive moment moves trailing edge down)

h_t tab section hinge moment about tab hinge axis (positive moment moves trailing edge down)

c chord of basic airfoil with flap and tab neutral

c_f flap chord from flap hinge axis to trailing edge

c_t tab chord from tab hinge axis to trailing edge

q free-stream dynamic pressure

p_L static pressure on lower surface of seal

p_U static pressure on upper surface of seal

c_b balance chord

α_o angle of attack for airfoil of infinite aspect ratio (positive when nose of airfoil moves up)

δ_f flap deflection with respect to airfoil (positive when trailing edge is deflected downward)

δ_t tab deflection with respect to flap (positive when trailing edge is deflected downward)

also

$$a_{\delta_f} = \left(\frac{\partial a_o}{\partial \delta_f}\right)_{c_l, \delta_t}$$

$$c_{l_a} = \left(\frac{\partial c_l}{\partial a_o}\right)_{\delta_f, \delta_t}$$

$$c_{l_{\delta_f}} = \left(\frac{\partial c_l}{\partial \delta_f}\right)_{a_o, \delta_t}$$

$$c_{h_{f_a}} = \left(\frac{\partial c_{h_f}}{\partial a_o}\right)_{\delta_f, \delta_t}$$

$$c_{h_{f_{\delta_f}}} = \left(\frac{\partial c_{h_f}}{\partial \delta_f}\right)_{a_o, \delta_t}$$

$$\left(c_{m_{c_l}}\right)_{\delta_f, \delta_t} = \left(\frac{\partial c_m}{\partial c_l}\right)_{\delta_f, \delta_t}$$

$$\left(c_{m_{c_l}}\right)_{a_o, \delta_t} = \left(\frac{\partial c_m}{\partial c_l}\right)_{a_o, \delta_t}$$

The subscripts outside the parentheses represent the factors held constant during the measurement of the parameters.

APPARATUS AND MODEL

The tests were conducted in the Langley 4- by 6-foot vertical tunnel described in reference 1 and modified as described in reference 2.

The model, when mounted in the tunnel, spanned the test section except for clearances of 1/32 inch between the model and the tunnel walls. With this type of installation, two-dimensional flow is closely approximated and the section characteristics of the airfoil, the flap, and the tab may be determined. The model was attached to the balance frame by torque tubes that extended through the sides of the tunnel. The angle of

attack was set from outside the tunnel by rotating the torque tubes with an electric drive. Flap deflections were set by means of an electrical position indicator and tab deflections were set with a templet. The hinge moments of the flap were measured with a special torque-rod balance built into the model. For the tab tests, tab hinge moments were taken by an electrical strain gage installed in the model. For the plain sealed flap, the pressure difference across the seal of the gap at the flap nose was measured on a manometer.

The 2-foot-chord by 4-foot-span model (fig. 1) was constructed of laminated mahogany (except for a steel tab), was aerodynamically smooth, and was made to conform to the NACA 0009 profile (table I). It was equipped with a 0.40c flap and a $0.20c_f$ plain tab.

The flap had a plain-nose overhang with a radius of approximately one-half of the airfoil thickness at the flap hinge axis and was so constructed that it could be fitted with aerodynamic balances that were 35 and 50 percent of the flap chord. These balances were of blunt and elliptical nose shape. The elliptical nose was a true ellipse faired tangent to the airfoil contour at the flap hinge axis. The ordinates for the elliptical-nose overhang are given in table II. The nose radii shown in figure 1 determined the blunt and plain nose shapes. The various overhangs consisted of nose blocks that could be attached interchangeably to the flap at the hinge axis. In order to keep the 0.005c gap at the flap nose (flap gap) constant, these nose blocks were matched by interchangeable blocks in the airfoil just forward of the flap. An airtight fabric connected the flap nose and the forward part of the airfoil for the sealed-gap tests.

The $0.20c_f$ tab was made of steel and the nose radius was approximately one-half of the airfoil thickness at the tab hinge axis. The gap at the tab nose (tab gap) was 0.001c.

TESTS

In order that the test results may be found easily, the various flap configurations tested and the figure numbers of the corresponding plotted data are given in table III.

The tests were made at a dynamic pressure of 13 pounds per square foot, which corresponds to a velocity of about 71 miles per hour at standard sea-level conditions. The test Reynolds number was about 1,330,000. Since the tunnel turbulence factor is 1.93, the effective Reynolds number was approximately 2,570,000. The Mach number for these tests was about 0.09.

The maximum error in angle of attack appears to be $\pm 0.2^{\circ}$. It is estimated that the flap and tab deflections were set to within $\pm 0.2^{\circ}$.

An experimentally determined tunnel correction was applied to the lift. The angle of attack and hinge moments were corrected for the effect of streamline curvature induced by the tunnel walls. The method used to determine these corrections is similar to the theoretically derived analysis presented in reference 3 for finite-span models. The increments of drag are thought to be reasonably independent of tunnel effect, although the absolute values are subject to an undetermined correction. Inaccuracy in the model construction and in the assembly of the interchangeable blocks probably caused the small amount of flap hinge moment at zero angle of attack and flap deflection.

DISCUSSION

Lift

The lift-coefficient curves for the flap with a plain overhang and with aerodynamic balance are shown in figures 2 to 11. With the gap either sealed or unsealed, the lift-coefficient curves were nonlinear at large flap deflections.

The slope of the lift-coefficient curve c_{l_α} (table IV) was approximately the same with gap sealed for all flap arrangements regardless of aerodynamic-balance shape or length except for the $0.50c_f$ elliptical-nose overhang for which the slope was about 3 percent larger than the average. Unsealing the gap caused a 4-percent reduction in slope for the flap with a plain overhang and a 13- to 17-percent reduction for the flap with blunt and elliptical overhangs. For a given balance

chord and with gap sealed, c_{l_α} was approximately the same regardless of nose shape.

The change in lift with flap deflection $c_{l_{\delta_f}}$ increased when the flap gap was sealed and when the nose shape was changed from elliptical to blunt. The flap lift effectiveness α_{δ_f} varied in a similar manner except that, in the case of the $0.50c_f$ blunt-nose overhang, α_{δ_f} decreased when the gap was sealed. It should be remembered that the parameters shown in table IV were measured over a small flap-deflection range (0° to 5°) and therefore are used mainly to compare the various flap configurations tested.

Hinge Moment

The curves of flap hinge-moment coefficient as a function of angle of attack at a constant flap deflection for the flap with plain and balanced overhangs are also presented in figures 2 to 11.

For the $0.50c_f$ blunt overhang with gap both sealed and unsealed and the $0.50c_f$ elliptical overhang with gap unsealed, the aerodynamic characteristics at large flap deflections were not determined because of violent oscillations that might have damaged the tunnel apparatus. Ranges in which oscillations occurred are noted by dashed lines in the hinge-moment curves. Similar oscillations encountered on another flap fitted with an aerodynamic balance are discussed in reference 4.

The hinge-moment parameters presented in table IV indicate that an overbalance condition occurred for the $0.50c_f$ blunt-nose overhang with gap either sealed or unsealed. The $0.50c_f$ elliptical overhang had a positive $c_{h_{f_\alpha}}$ for both gap conditions and had small negative values of $c_{h_{f_{\delta_f}}}$ for small flap deflections to about 5° (figs. 10 and 11).

When section data are applied to finite spans, the aspect-ratio corrections for streamline curvature are always positive (reference 5). Since the hinge-moment

parameters for several arrangements of the flap with balanced overhangs are very small and the signs critical, the slopes may pass through zero and an overbalanced flap may result.

The effect of sealing the flap gap was to make $c_{h_{f_\alpha}}$ and $c_{h_{f_{\delta_f}}}$ more negative except that, with the flap having a plain overhang, the opposite effect occurred. Increasing the balance length made both $c_{h_{f_\alpha}}$ and $c_{h_{f_{\delta_f}}}$ more positive. For a given balance chord, greater balance was obtained at small flap deflections with the blunt nose than with the elliptical nose. Examination of the curves shows, however, that, at large flap deflections for the $0.35c_f$ overhang, the elliptical-nose overhang had the greater balancing effect. The variation of the hinge-moment parameters with overhang for the elliptical and blunt nose is shown in figure 12.

Because the hinge-moment parameters shown in table IV and figure 12 represent the slopes of the curves at zero flap deflection and angle of attack, these parameters should be used mainly as an indication of the relative merits of the different flap nose shapes. Because the tabulated slopes are valid for only small ranges, the slopes from the hinge-moment-coefficient curves rather than the values of table IV should be used in calculating the characteristics of a control surface.

The present investigation did not include tests to determine the effect on flap hinge moment of sealing the tab gap. It is thought that the flap hinge moments for a flap without a tab (or with tab gap sealed) might vary somewhat from the flap hinge moments of the model configurations tested with tab gap unsealed.

Pitching Moment

The values of the pitching-moment parameters $(c_{m_{c_l}})_{\delta_f,\delta_t}$ and $(c_{m_{c_l}})_{\alpha_o,\delta_t}$ in table IV determine the position of the center of lift with respect to the quarter-chord point of the airfoil. When lift was varied by changing the angle of attack with a flap deflection of 0°, the center

of lift was at approximately the 0.24c station for all overhangs tested with gap sealed. Unsealing the gap had no effect on the center of lift of the plain flap but moved the center of lift rearward to the 0.25c station for the 0.35c overhang and rearward to the 0.26c station for the 0.50c overhang.

The following table gives the position of the center of lift caused by flap deflection:

Flap gap	Position of center of lift caused by flap deflection				
	Plain overhang	$0.35c_f$ overhang		$0.50c_f$ overhang	
		Blunt nose	Elliptical nose	Blunt nose	Elliptical nose
Sealed	0.37c	0.38c	0.37c	0.39c	0.38c
0.005c	.38c	.39c	.43c	.38c	.41c

These data indicate that the center of lift generally moved rearward as the flap gap was unsealed. Increasing the balance chord and changing the nose shape from elliptical to blunt moved the center of lift rearward for the sealed-gap condition and forward for the unsealed-gap condition.

The position of the center of lift caused by flap deflection is a function of the aspect ratio (references 5 and 6) and moves toward the trailing edge as the aspect ratio decreases.

Drag

Because of an undetermined tunnel correction, the measured values of drag cannot be considered accurate; relative drag values are thought to be reasonably independent of tunnel effect and were therefore used. The smallest percentage increase in profile-drag coefficient caused at zero angle of attack and flap deflection by replacing the plain flap with a flap with balanced overhang was obtained with the blunt-nose overhangs. The increase in c_{d_0} ranged from 0.0006

for the $0.35c_f$ overhang with flap gap sealed to 0.0017 for the $0.50c_f$ overhang with flap gap sealed. The $0.50c_f$ elliptical overhang with flap gap sealed had the largest increase (0.0037) in c_{d_o} over that for the airfoil with the plain flap.

The increments of profile-drag coefficient caused by flap deflection Δc_{d_o} for the flap with a plain overhang (fig. 13) were generally larger with the gap open than with the gap sealed. Since the blunt-nose overhang gave smaller increments of drag than the elliptical-nose overhang at small flap deflections - such as may be necessary for the trim change - the increments of drag are presented for only the $0.35c_f$ and $0.50c_f$ blunt-nose overhangs (figs. 14 and 15, respectively). For the $0.35c_f$ blunt-nose overhang, lower increments of drag occurred with gap unsealed than with gap sealed. The $0.50c_f$ blunt-nose overhang had lower increments of drag with gap sealed except that, at an angle of attack of 8°, the increments were larger with gap sealed than with gap unsealed.

Tab Characteristics

Only a limited investigation of tab characteristics has been made because the tab characteristics of a flap with aerodynamic balance are generally independent of flap nose shape (reference 7) and are similar to those for a tab on a plain flap (references 2 and 7). The present investigation included tests of balancing and unbalancing tabs on the plain sealed flap (fig. 16) and on the sealed flap with the $0.35c_f$ elliptical overhang (fig. 17) with $\frac{\partial \delta_t}{\partial \delta_f} = -1$ and 1. For the tests with balancing tabs, $\frac{\partial \delta_t}{\partial \delta_f} = -1$ was found to be too large since some overbalance occurred.

The flap with the $0.50c_f$ blunt-nose overhang, which was found to be overbalanced throughout most of the deflected range, could be modified by using a tab deflected in the same direction as the flap. This arrangement should increase the lift effectiveness and provide the desired hinge moments. No data have been obtained for this condition, however.

Pressure Difference across the Plain Flap Seal

The variation of resultant pressure coefficient across the seal of the plain-flap nose with angle of attack at a constant flap deflection is shown in figure 18. The change in resultant pressure coefficient with angle of attack $\left(\frac{\partial P_R}{\partial \alpha_o}\right)_{\delta_f,\delta_t}$ was generally found to increase with increasing flap deflection.

The resultant pressure coefficient of the plain flap is useful in determining hinge-moment coefficients of flaps with internal balances. It can be shown that

$$\left(c_{h_f}\right)_{I.B.} = c_{h_f} + P_R K \qquad (1)$$

where

$\left(c_{h_f}\right)_{I.B.}$ section hinge-moment coefficient for flap with internal balance

c_{h_f} section hinge-moment coefficient for plain flap with gap sealed

P_R resultant pressure coefficient

$K = \dfrac{(c_b/c_f)^2 - (t/c_f)^2}{2}$ (see fig. 19)

t semithickness at hinge

The data of figure 18 can be used with that of figure 3 to determine the flap section hinge-moment coefficient at a given angle of attack and flap deflection for a 0.40c flap with an internal balance on an NACA 0009 airfoil. The values of K are presented in figure 19 as a function of balance chord. Hinge-moment parameters c_{h_α} and $c_{h_{\delta_f}}$ determined from hinge-moment coefficients obtained by equation (1) are presented for various lengths of internal balance in figure 12.

CONCLUSIONS

The results of tests of an NACA 0009 airfoil with a 40-percent-chord flap having various arrangements of overhang and nose shape indicate the following conclusions:

1. The slope of the lift-coefficient curve was approximately the same for all sealed-gap conditions regardless of aerodynamic-balance shape or length, except for the elliptical-nose overhang with a 50-percent-flap chord for which the slope was about 3 percent larger than the average. Unsealing the gap reduced the slope 4 percent for the flap with plain overhang and 13 to 17 percent for the flap with aerodynamic balances.

2. The change in lift with flap deflection increased with sealing of the flap gap and with changing of the nose shape from elliptical to blunt.

3. Unsealing the flap gap (except for the plain flap), increasing the balance length, and changing the nose shape from elliptical to blunt made the rate of change of flap hinge moment with flap deflection (at small flap deflections) and with angle of attack more positive (or less negative).

4. With gap either sealed or unsealed, some overbalance was found on the 50-percent-chord blunt-nose overhang.

5. When the lift was varied by changing the angle of attack at zero flap deflection, the center of lift was at the 24-percent-chord station (0.24c) for all overhangs tested with gap sealed.

6. The center of lift due to flap deflection and that due to angle of attack generally moved rearward as the gap was unsealed.

Langley Memorial Aeronautical Laboratory
National Advisory Committee for Aeronautics
Langley Field, Va.

REFERENCES

1. Wenzinger, Carl J., and Harris, Thomas A.: The Vertical Wind Tunnel of the National Advisory Committee for Aeronautics. NACA Rep. No. 387, 1931.

2. Sears, Richard I., and Hoggard, H. Page., Jr.: Wind-Tunnel Investigation of Control-Surface Characteristics. VII - A Medium Aerodynamic Balance of Two Nose Shapes Used with a 30-Percent-Chord Flap on an NACA 0015 Airfoil. NACA ARR, July 1942.

3. Swanson, Robert S., and Toll, Thomas A.: Jet-Boundary Corrections for Reflection-Plane Models in Rectangular Wind Tunnels. NACA ARR No. 3E22, 1943.

4. Rogallo, F. M., and Purser, Paul E.: Wind-Tunnel Investigation of 20-Percent-Chord Plain and Frise Ailerons on an NACA 23012 Airfoil. NACA ARR, Dec. 1941.

5. Swanson, Robert S., and Gillis, Clarence L.: Limitations of Lifting-Line Theory for Estimation of Aileron Hinge-Moment Characteristics. NACA CB No. 3L02, 1943.

6. Ames, Milton B., Jr., and Sears, Richard I.: Determination of Control-Surface Characteristics from NACA Plain-Flap and Tab Data. NACA Rep. No. 721, 1941.

7. Ames, Milton B., Jr.: Wind-Tunnel Investigation of Control-Surface Characteristics. III - A Small Aerodynamic Balance of Various Nose Shapes Used with a 30-Percent-Chord Flap on an NACA 0009 Airfoil. NACA ARR, Aug. 1941.

TABLE I

ORDINATES FOR NACA 0009 AIRFOIL

[Stations and ordinates in percent of airfoil chord]

Station	Ordinates	
	Upper surface	Lower surface
0	0	0
1.25	1.42	-1.42
2.5	1.96	-1.96
5.0	2.67	-2.67
7.5	3.15	-3.15
10	3.51	-3.51
15	4.01	-4.01
20	4.30	-4.30
25	4.46	-4.46
30	4.50	-4.50
40	4.35	-4.35
50	3.97	-3.97
60	3.42	-3.42
70	2.75	-2.75
80	1.97	-1.97
90	1.09	-1.09
95	.60	-.60
100	(.10)	(-.10)
100	0	0
L.E. radius = 0.89		

TABLE II

STATIONS AND ORDINATES FOR ELLIPTICAL-NOSE

0.35c_f and 0.50c_f OVERHANGS

[Stations and ordinates are in percent chord; stations measured from leading edge of overhang]

0.35c_f overhang		0.50c_f overhang	
Station	Ordinate	Station	Ordinate
0	0	0	0
.03	.21	.03	.21
.10	.42	.11	.42
.20	.62	.25	.62
.35	.83	.45	.83
.54	1.04	.70	1.04
.79	1.25	1.02	1.25
1.08	1.46	1.40	1.46
1.43	1.67	1.86	1.67
1.83	1.88	2.40	1.88
2.31	2.08	3.02	2.08
2.87	2.29	3.75	2.29
3.53	2.50	4.61	2.50
4.31	2.71	5.62	2.71
5.26	2.92	6.84	2.92
6.47	3.12	8.36	3.12
8.21	3.33	10.46	3.33
11.63	3.49	15.79	3.54
14.01	3.42	20.00	3.42

TABLE III

FLAP CONFIGURATIONS TESTED

Overhang	Flap gap	Flap-deflection range (deg)	Tab gap	Tab-deflection range (deg)	Figure
Plain	0.005c	0 to 30	0.001c	0	2,13
Plain	Sealed	0 to 30	.001c	0	3,13
$0.35c_f$ blunt	0.005c	0 to 25	.001c	0	4,14
$0.35c_f$ blunt	Sealed	0 to 25	.001c	0	5,14
$0.35c_f$ elliptical	0.005c	0 to 25	.001c	0	6
$0.35c_f$ elliptical	Sealed	0 to 25	.001c	0	7
$0.50c_f$ blunt	0.005c	0 to 15	.001c	0	8,15
$0.50c_f$ blunt	Sealed	0 to 18	.001c	0	9,15
$0.50c_f$ elliptical	0.005c	0 to 20	.001c	0	10
$0.50c_f$ elliptical	Sealed	0 to 20	.001c	0	11
Plain	--do--	0 to 30	.001c	-30 to 30	16
$0.35c_f$ elliptical	--do--	0 to 20	.001c	-20 to 20	17

NATIONAL ADVISORY
COMMITTEE FOR AERONAUTICS

TABLE IV

PARAMETER VALUES FOR 0.40c FLAP WITH PLAIN, $0.35c_f$, AND $0.50c_f$ OVERHANGS ON NACA 0009 AIRFOIL

[Slopes were taken at zero flap deflection and angle of attack]

Nose shape	Flap gap	$c_{l_\alpha} = \left(\frac{\partial c_l}{\partial \alpha_o}\right)_{\delta_f,\delta_t}$	$c_{l_{\delta_f}} = \left(\frac{\partial c_l}{\partial \delta_f}\right)_{\alpha_o,\delta_t}$	$\alpha_{\delta_f} = \left(\frac{\partial \alpha_o}{\partial \delta_f}\right)_{c_l,\delta_t}$	$c_{h_{f_\alpha}} = \left(\frac{\partial c_{h_f}}{\partial \alpha_o}\right)_{\delta_f,\delta_t}$	$c_{h_{f_{\delta_f}}} = \left(\frac{\partial c_{h_f}}{\partial \delta_f}\right)_{\alpha_o,\delta_t}$	$\left(c_{m_{c_l}}\right)_{\delta_f,\delta_t} = \left(\frac{\partial c_m}{\partial c_l}\right)_{\delta_f,\delta_t}$	$\left(c_{m_{c_l}}\right)_{\alpha_o,\delta_t} = \left(\frac{\partial c_m}{\partial c_l}\right)_{\alpha_o,\delta_t}$
Plain overhang								
Plain	Sealed	0.100	0.068	-0.68	-0.0081	-0.0130	0.0050	-0.123
Plain	0.005c	.096	.064	-.66	-.0092	-.0136	.0052	-.135
$0.35c_f$ overhang								
Blunt	Sealed	0.098	0.070	-0.71	-0.0040	-0.0042	0.0092	-0.132
Blunt	0.005c	.083	.058	-.69	-.0014	-.0037	0	-.137
Elliptical	Sealed	.099	.062	-.63	-.0044	-.0061	.0131	-.116
Elliptical	0.005c	.083	.050	-.61	-.0020	-.0052	0	-.176
$0.50c_f$ overhang								
Blunt	Sealed	0.099	0.073	-0.71	0.0017	0.0073	0.0050	-0.145
Blunt	0.005c	.086	.072	-.80	.0125	.0084	-.0116	-.135
Elliptical	Sealed	.102	.065	-.66	.0006	-.0015	.0049	-.135
Elliptical	0.005c	.085	.053	-.58	.0058	-.0008	-.0059	-.160

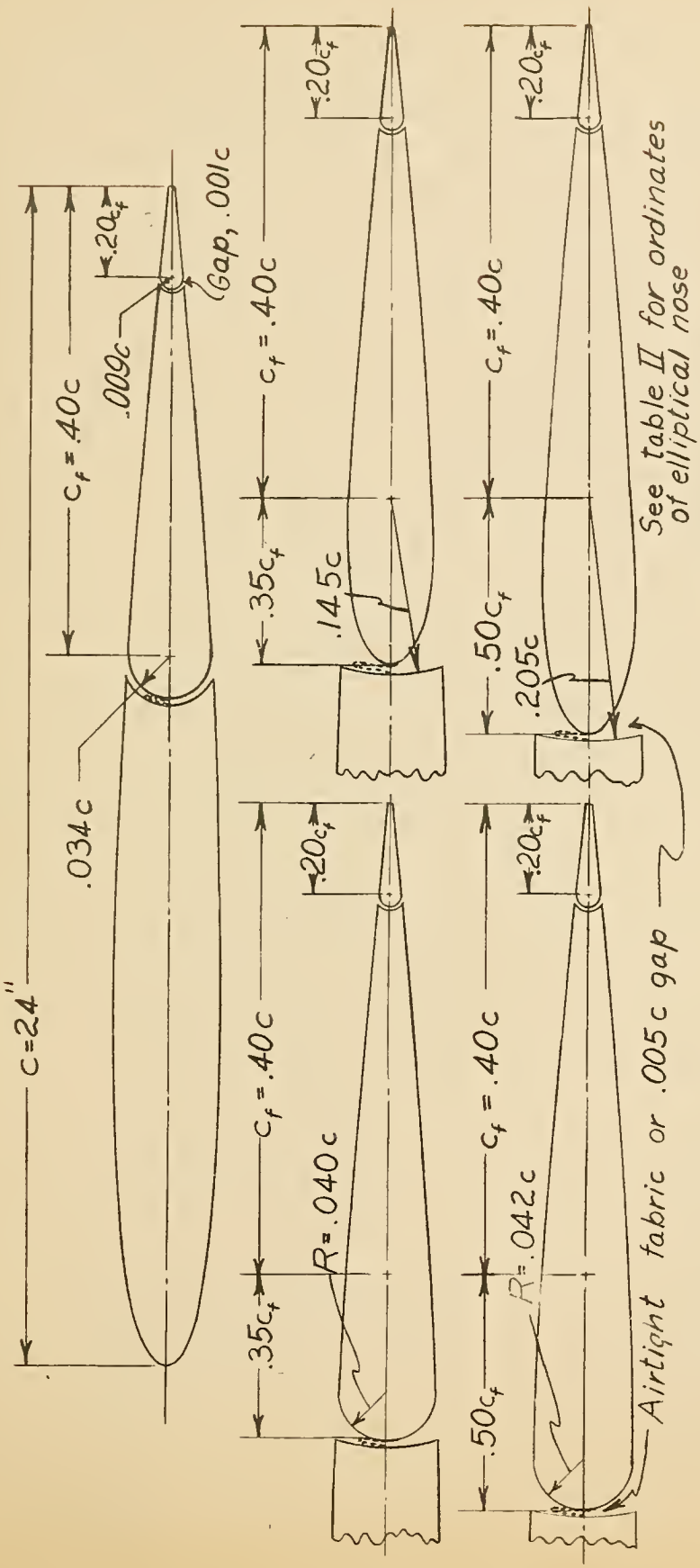

NATIONAL ADVISORY COMMITTEE FOR AERONAUTICS

Figure 1.- Nose shapes tested on a 0.40c flap with 0.35c_f and 0.50c_f blunt and elliptical overhangs on an NACA 0009 airfoil.

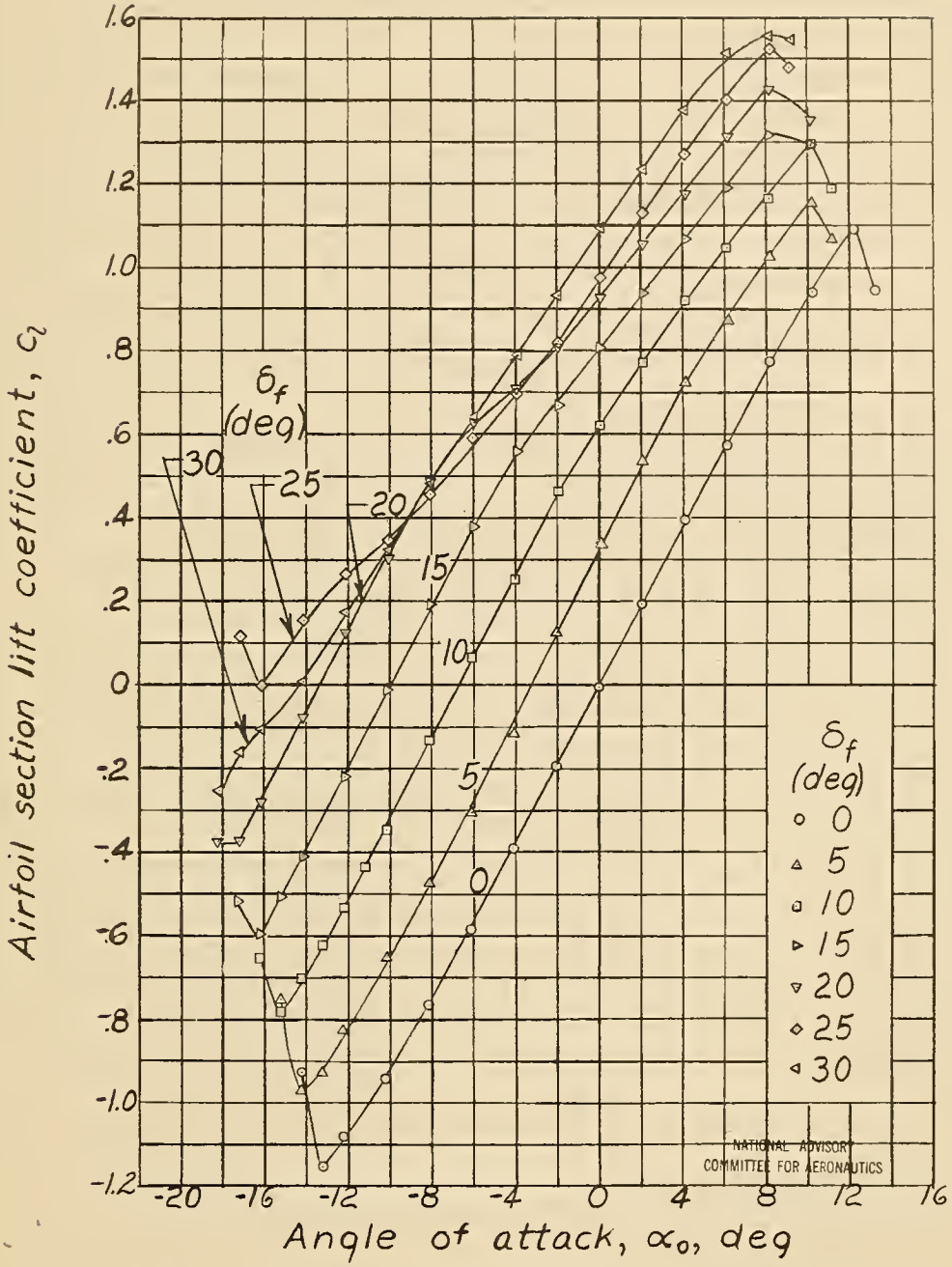

Figure 2. - Aerodynamic section characteristics of an NACA 0009 airfoil with a 0.40c plain flap. Flap gap, 0.005c; tab, 0.20c_f; tab gap, 0.001c; $\delta_t = 0°$.

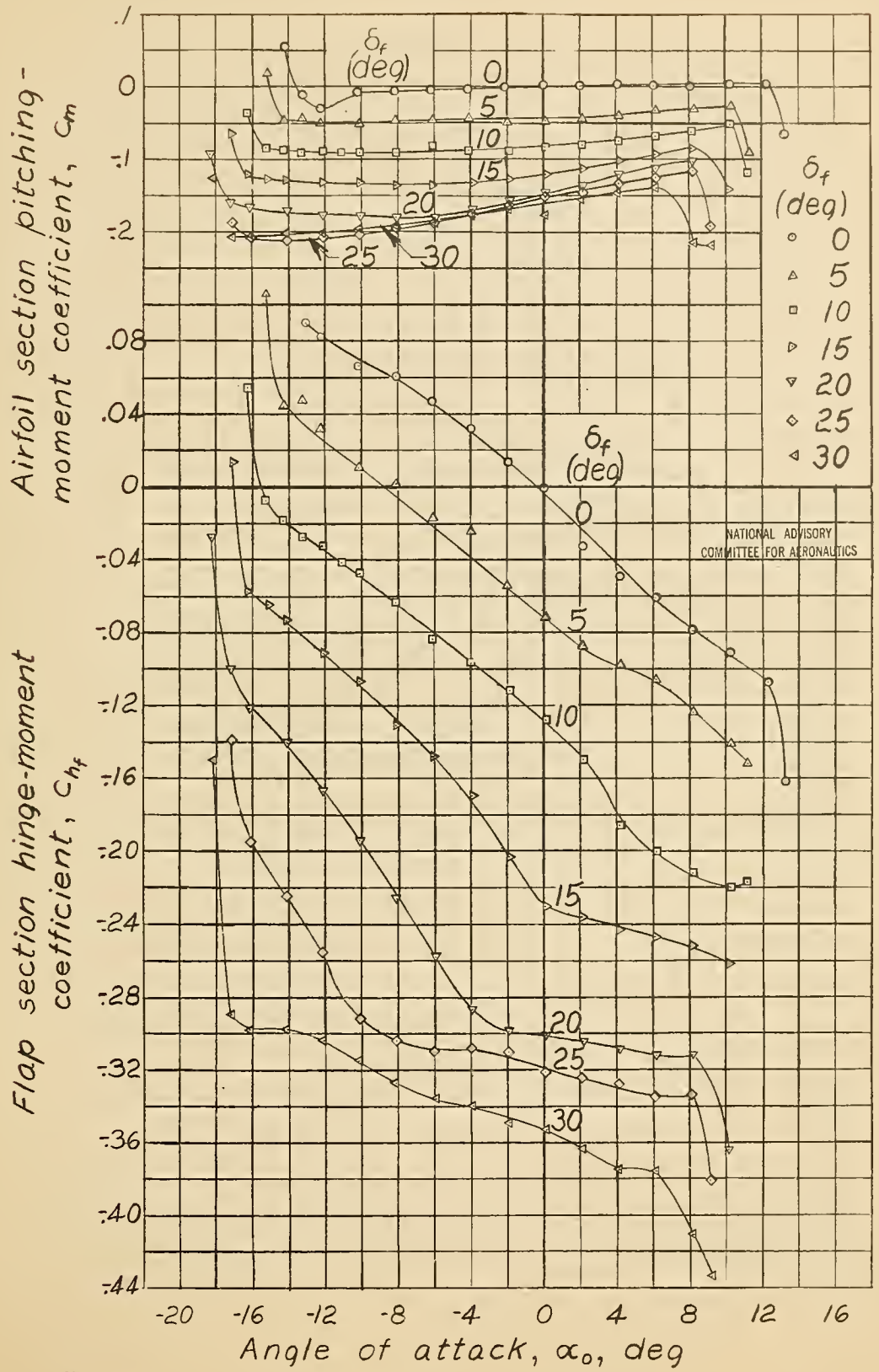

Figure 2.- Concluded.

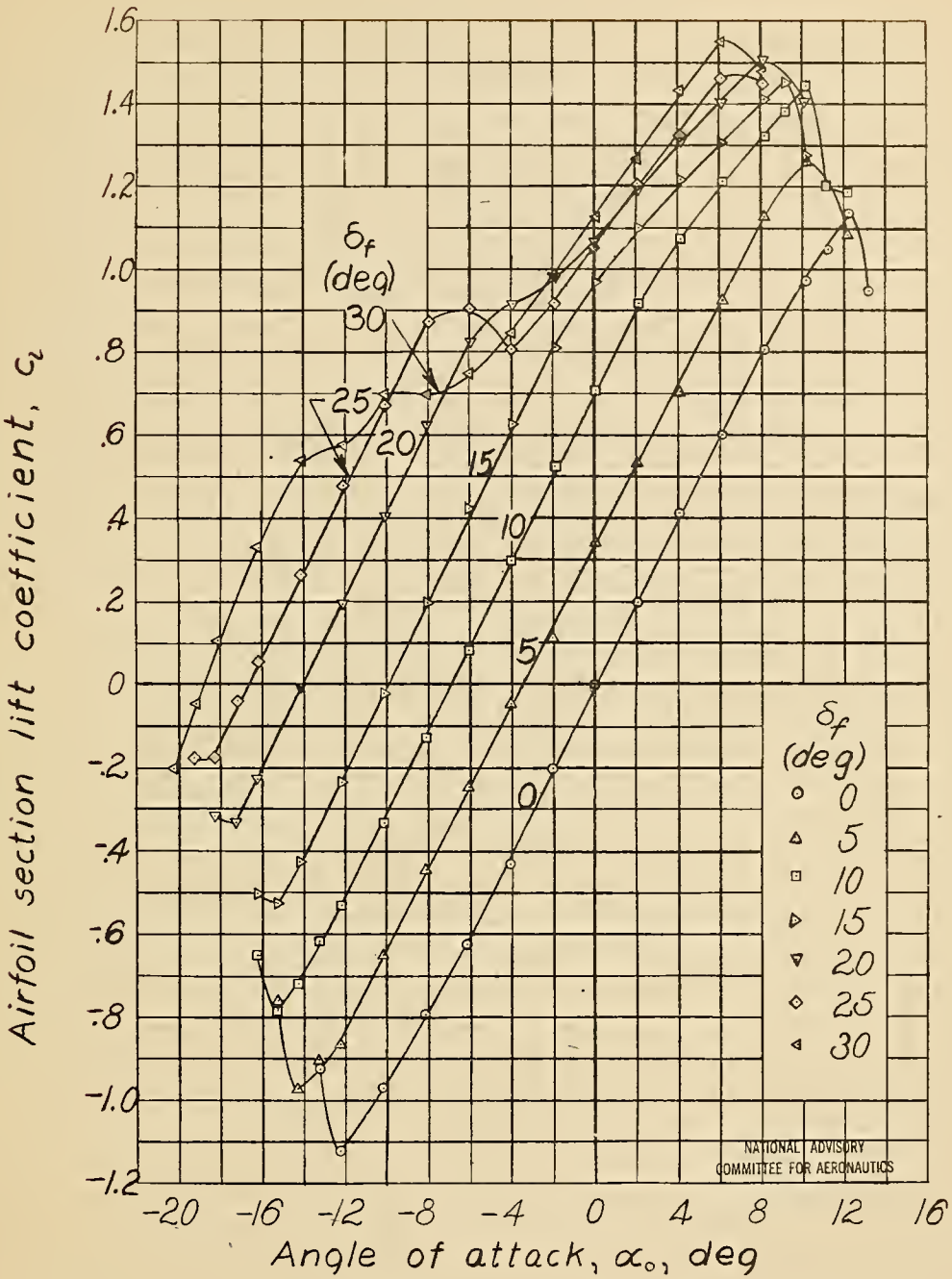

Figure 3. - Aerodynamic section characteristics of an NACA 0009 airfoil with a 0.40c plain flap. Flap gap sealed; tab, 0.20 c_f; tab gap, 0.001c; $\delta_t = 0°$.

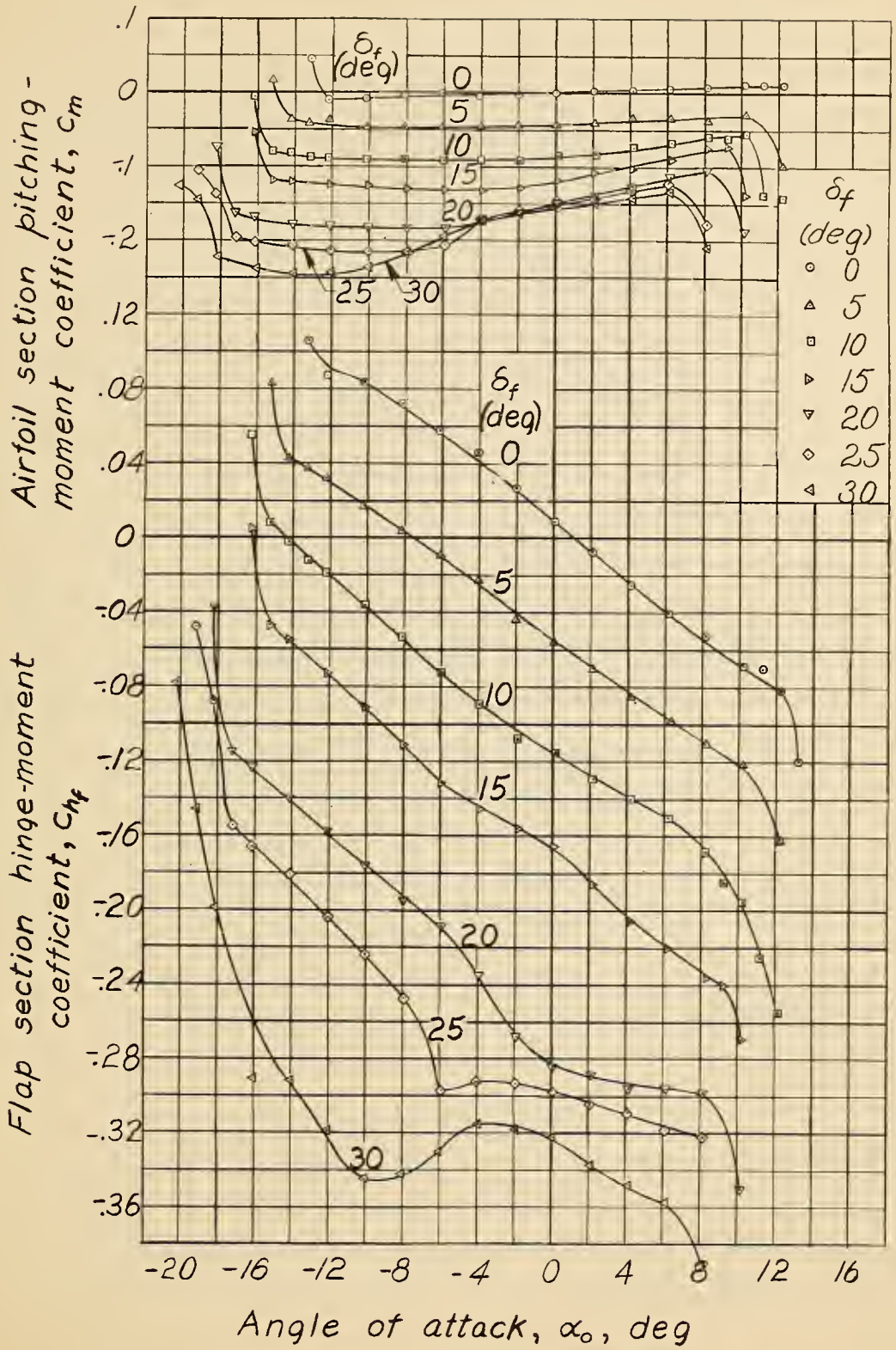

Figure 3. - Concluded.

NATIONAL ADVISORY COMMITTEE FOR AERONAUTICS

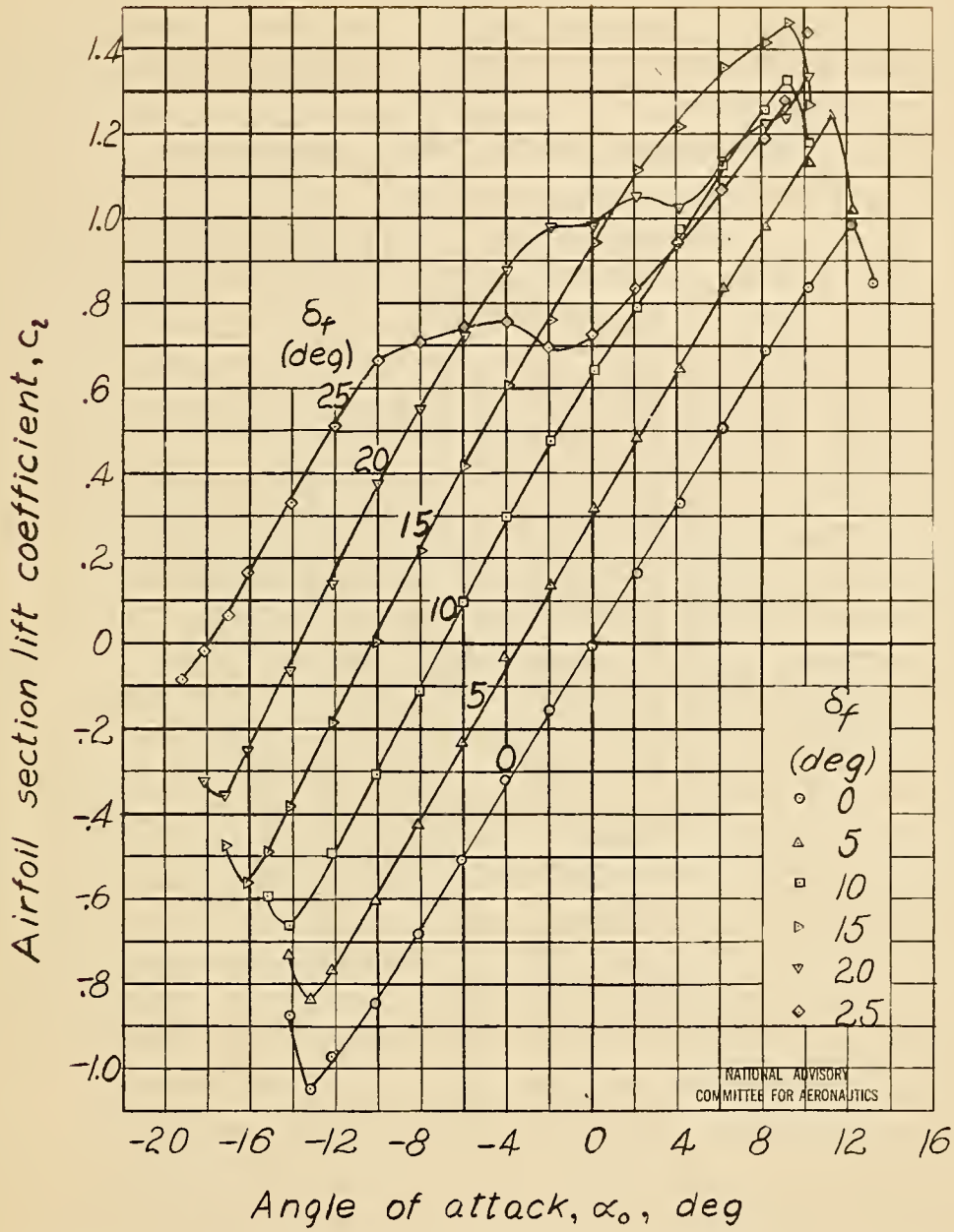

Figure 4.- Aerodynamic section characteristics of an NACA 0009 airfoil with a 0.40c flap having a 0.35c_f overhang with blunt nose. Flap gap, 0.005c; tab, 0.20 c_f; tab gap, 0.001c; $\delta_t = 0°$.

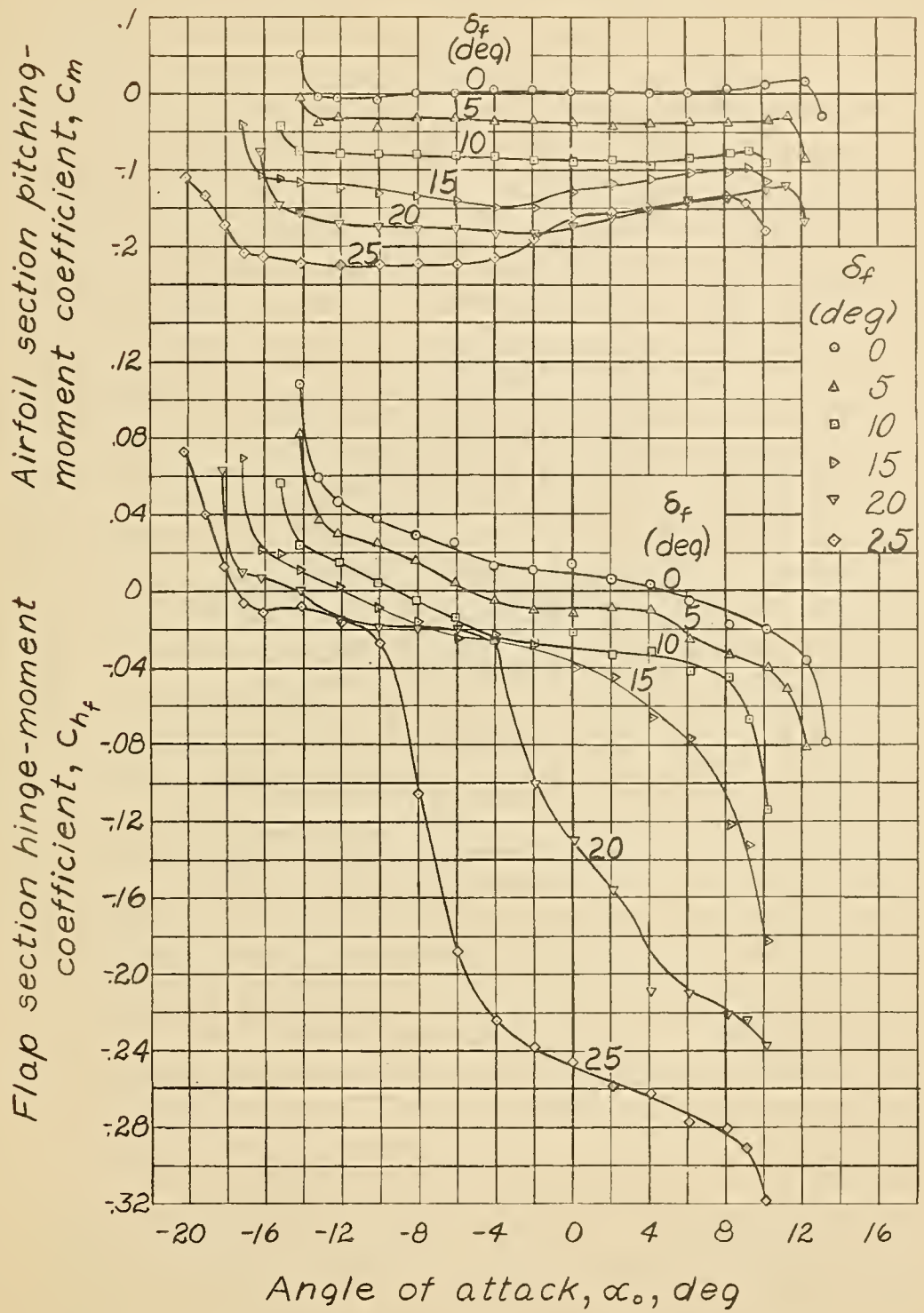

Figure 4.- Concluded.

NATIONAL ADVISORY COMMITTEE FOR AERONAUTICS

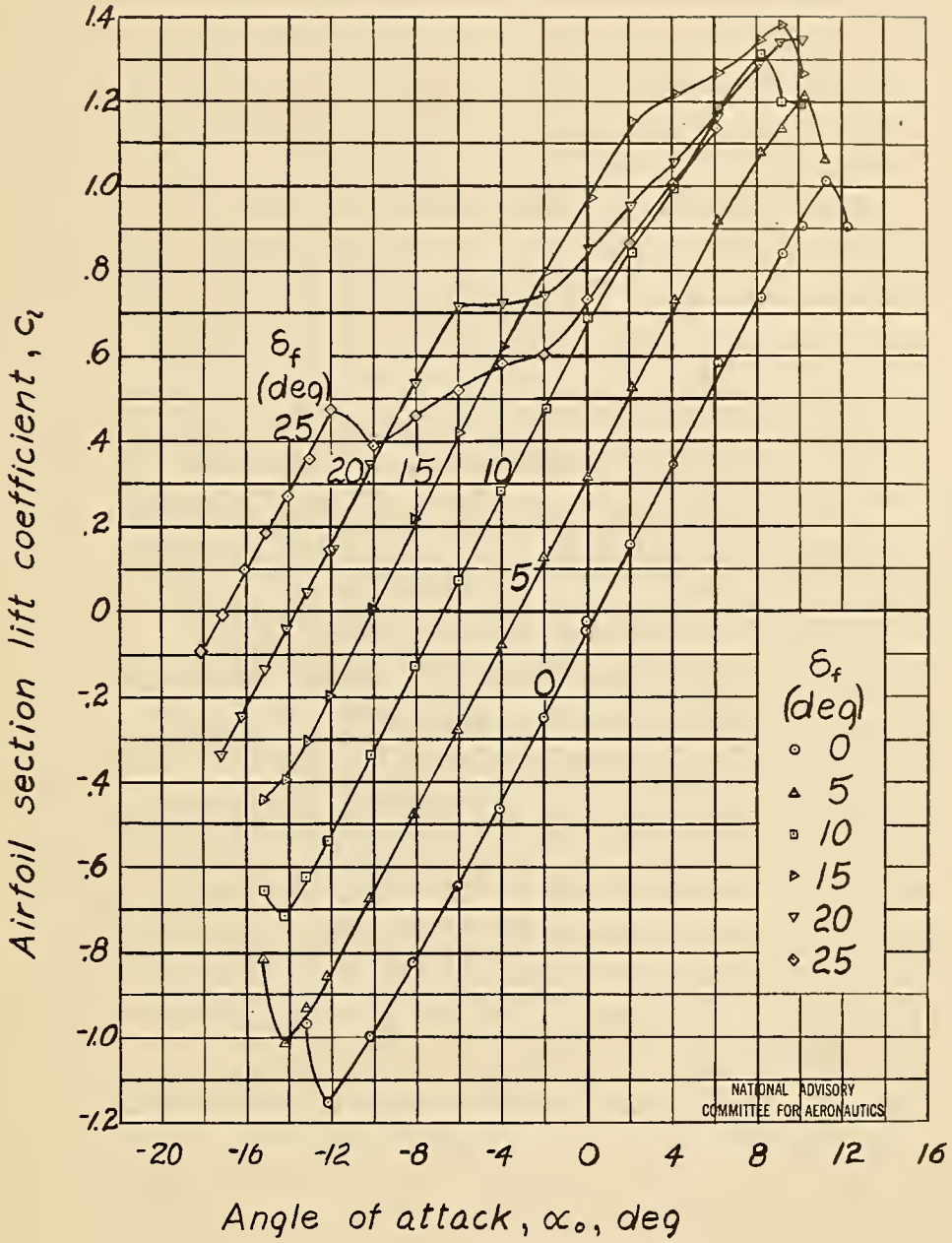

Figure 5.- Aerodynamic section characteristics of an NACA 0009 airfoil with a 0.40c flap having a 0.35c_f overhang with blunt nose. Flap gap sealed; tab, 0.20c_f; tab gap, 0.001c; δ_t = 0°.

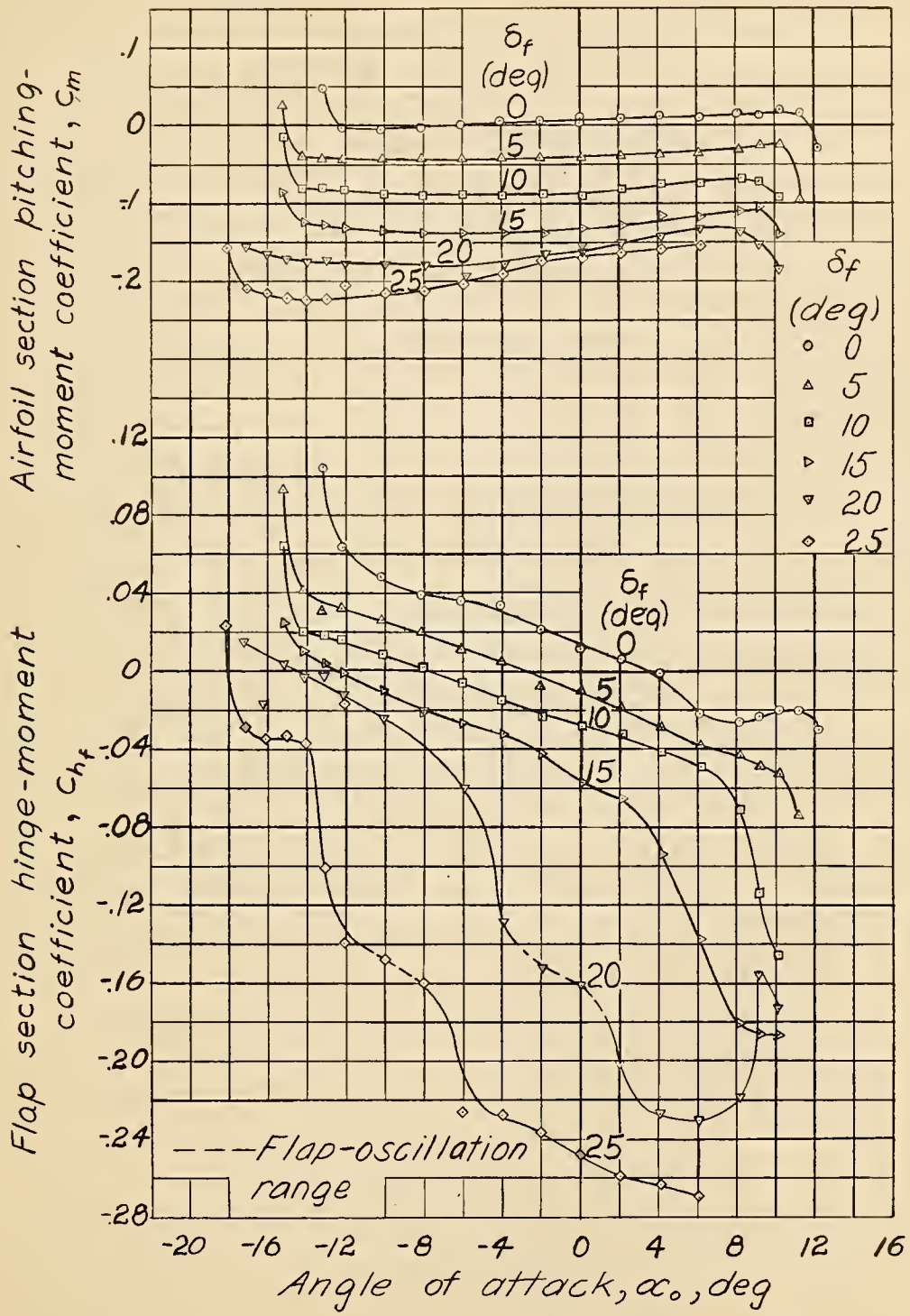

Figure 5.- Concluded.

NATIONAL ADVISORY COMMITTEE FOR AERONAUTICS

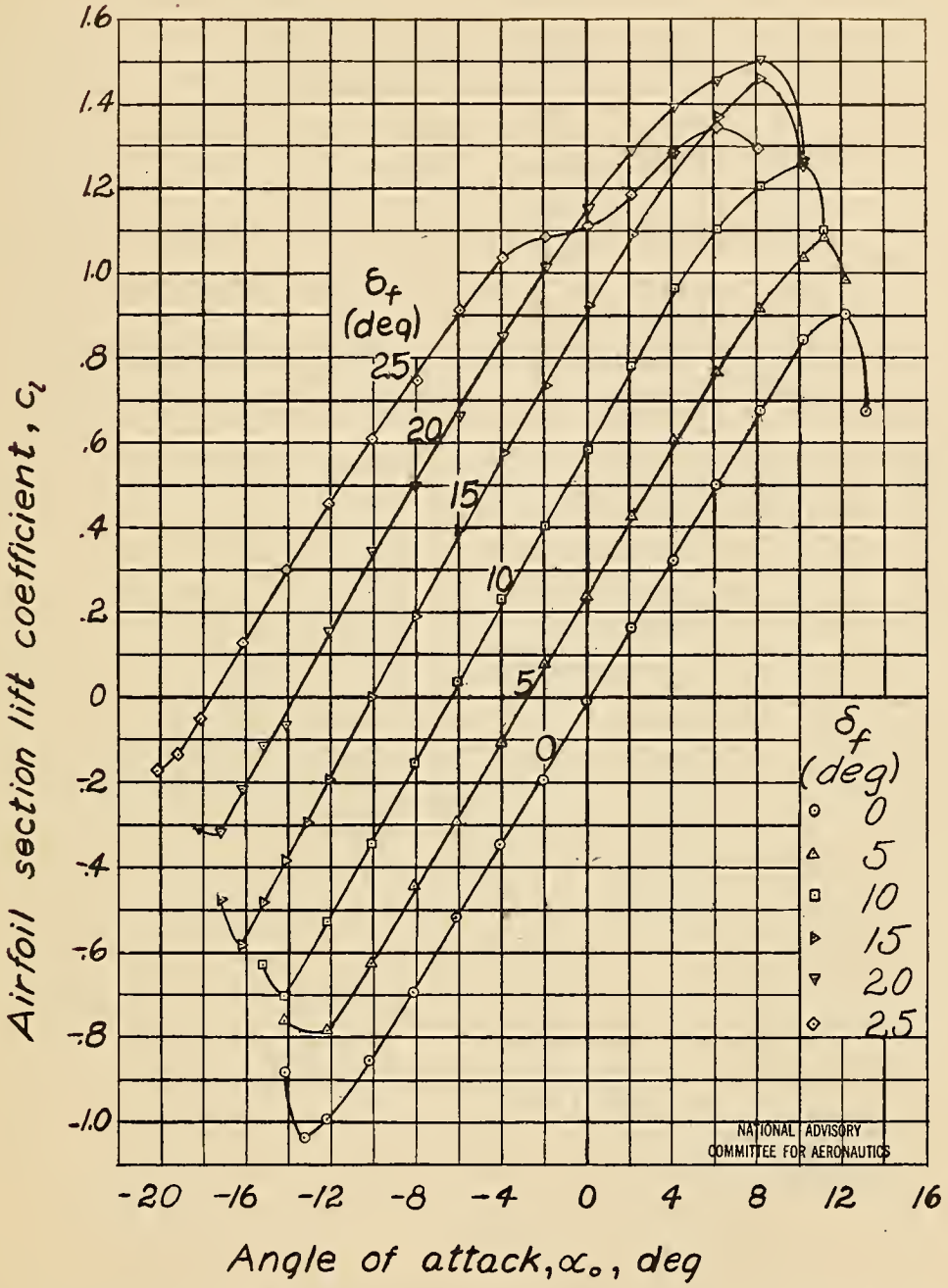

Figure 6.-Aerodynamic section characteristics of an NACA 0009 airfoil with a 0.40c flap having a 0.35c_f overhang with elliptical nose. Flap gap, 0.005c; tab, 0.20c_f; tab gap, 0.001c; $\delta_t = 0°$.

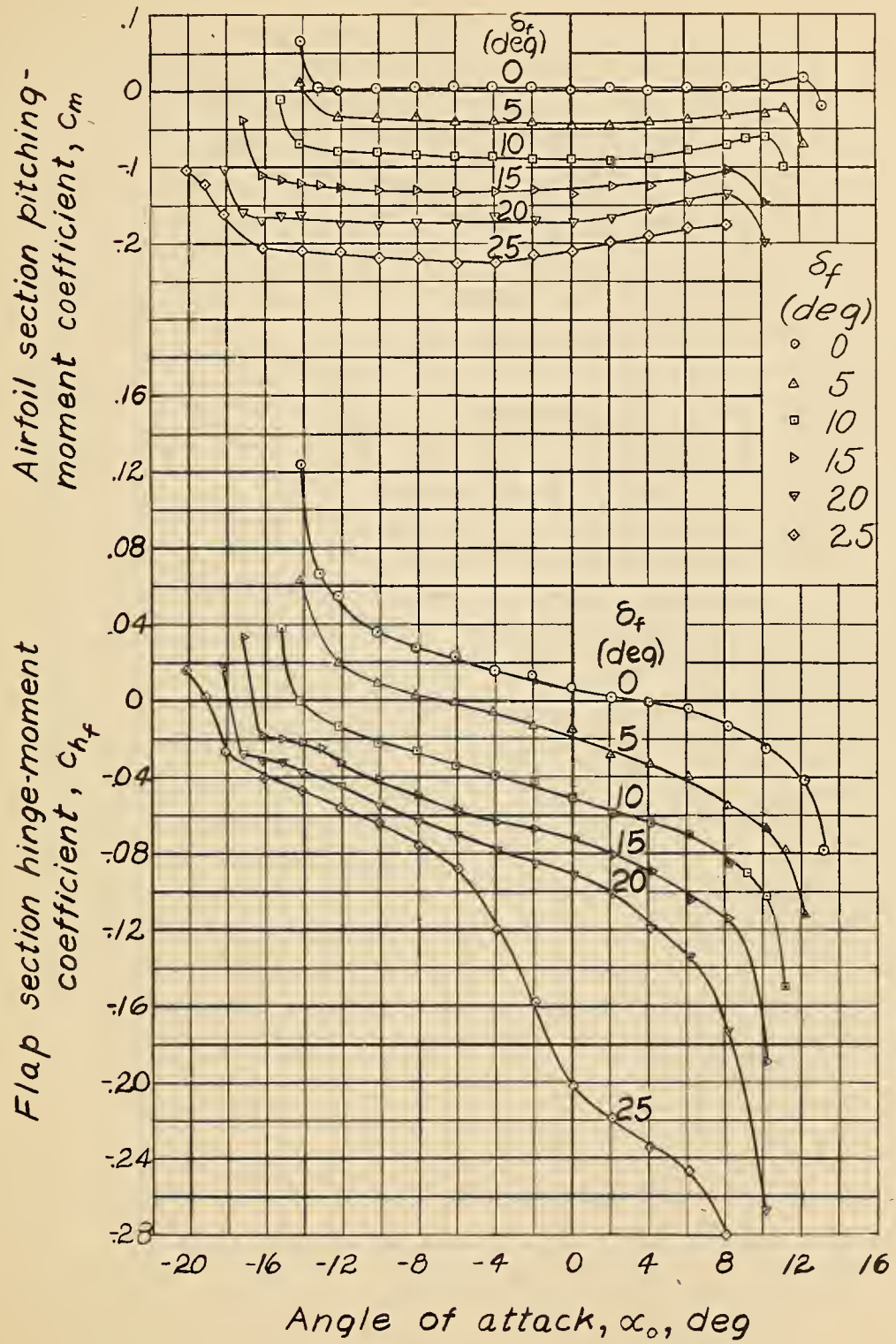

Figure 6.-Concluded.

NATIONAL ADVISORY COMMITTEE FOR AERONAUTICS

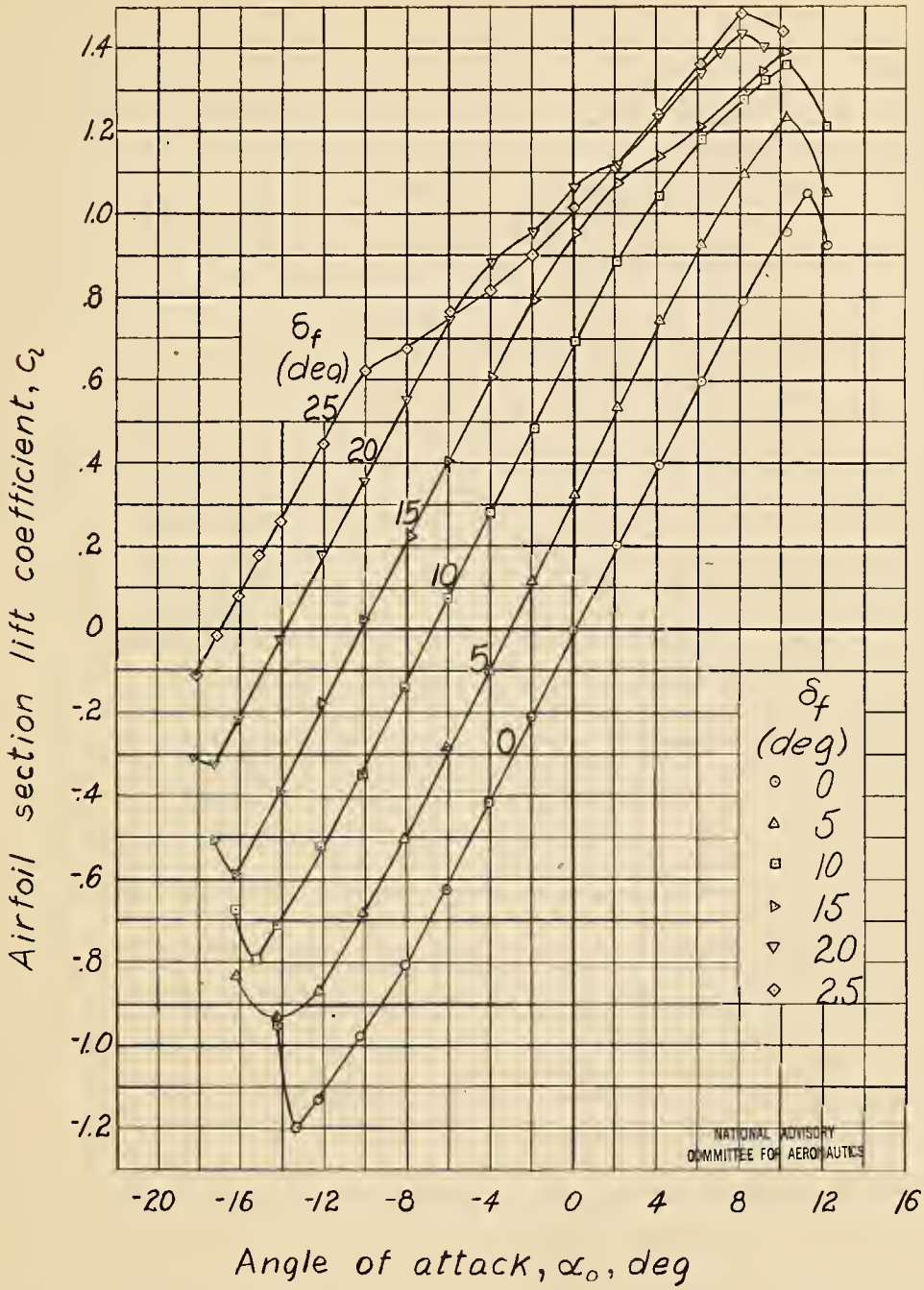

Figure 7.- Aerodynamic section characteristics of an NACA 0009 airfoil with a 0.40c flap having a 0.35c_f overhang with elliptical nose. Flap gap sealed; tab, 0.20 c_f; tab gap, 0.001c; $\delta_t = 0°$.

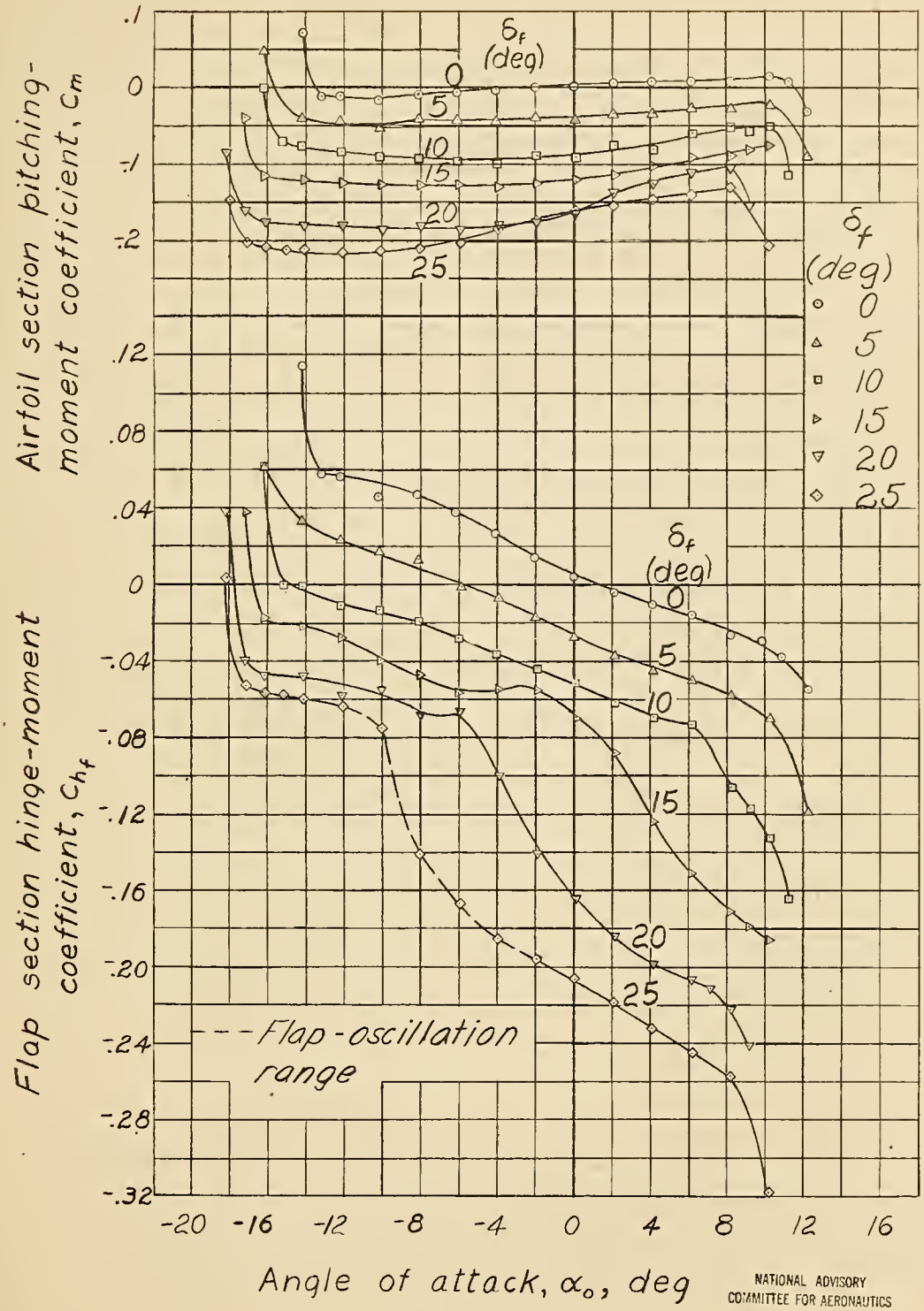

Figure 7. - Concluded.

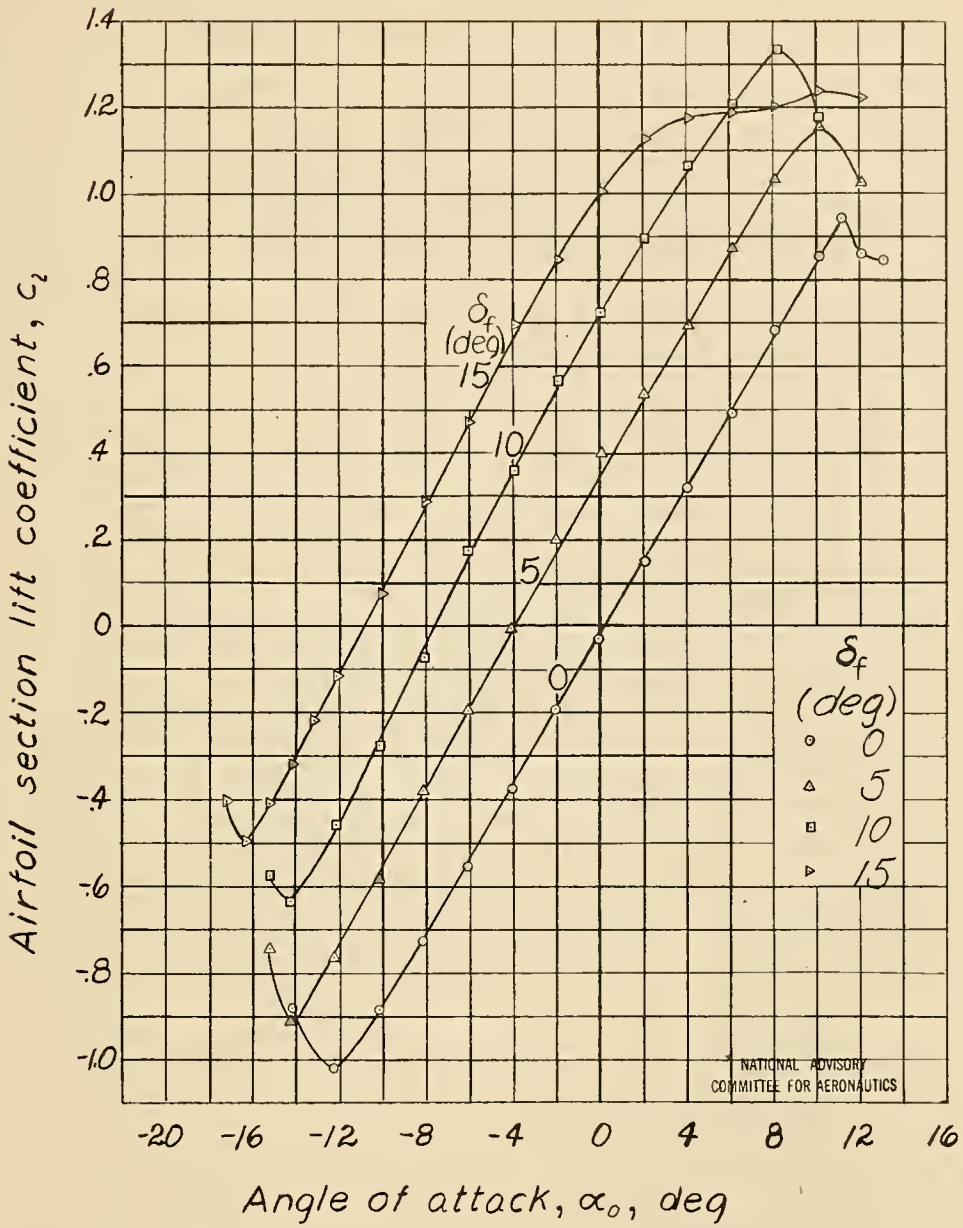

Figure 8.- Aerodynamic section characteristics of an NACA 0009 airfoil with a 0.40c flap having a 0.50c_f overhang with blunt nose. Flap gap, 0.005c; tab, 0.20c_f; tab gap, 0.001c; $\delta_t = 0°$.

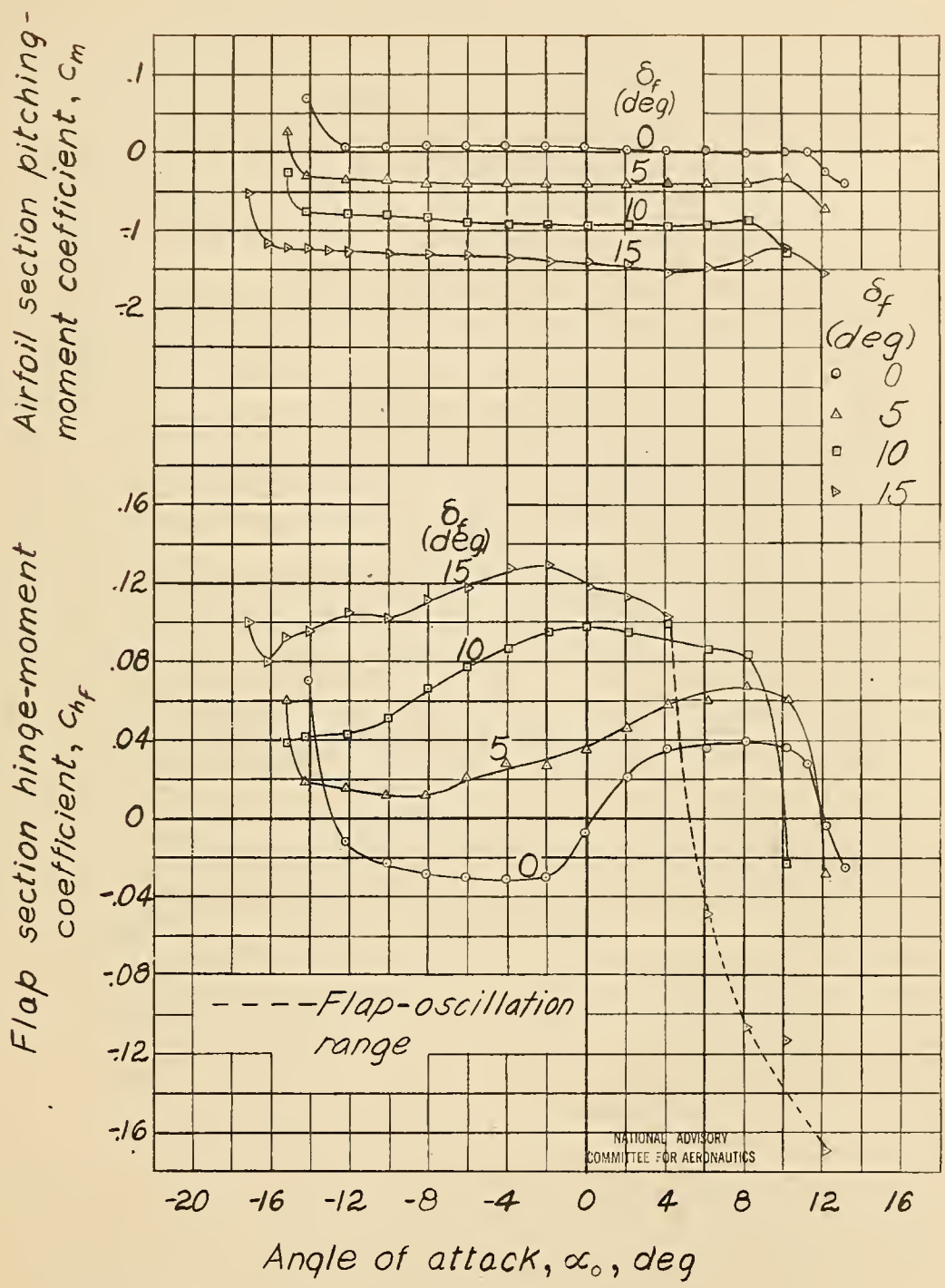

Figure 8. - Concluded.

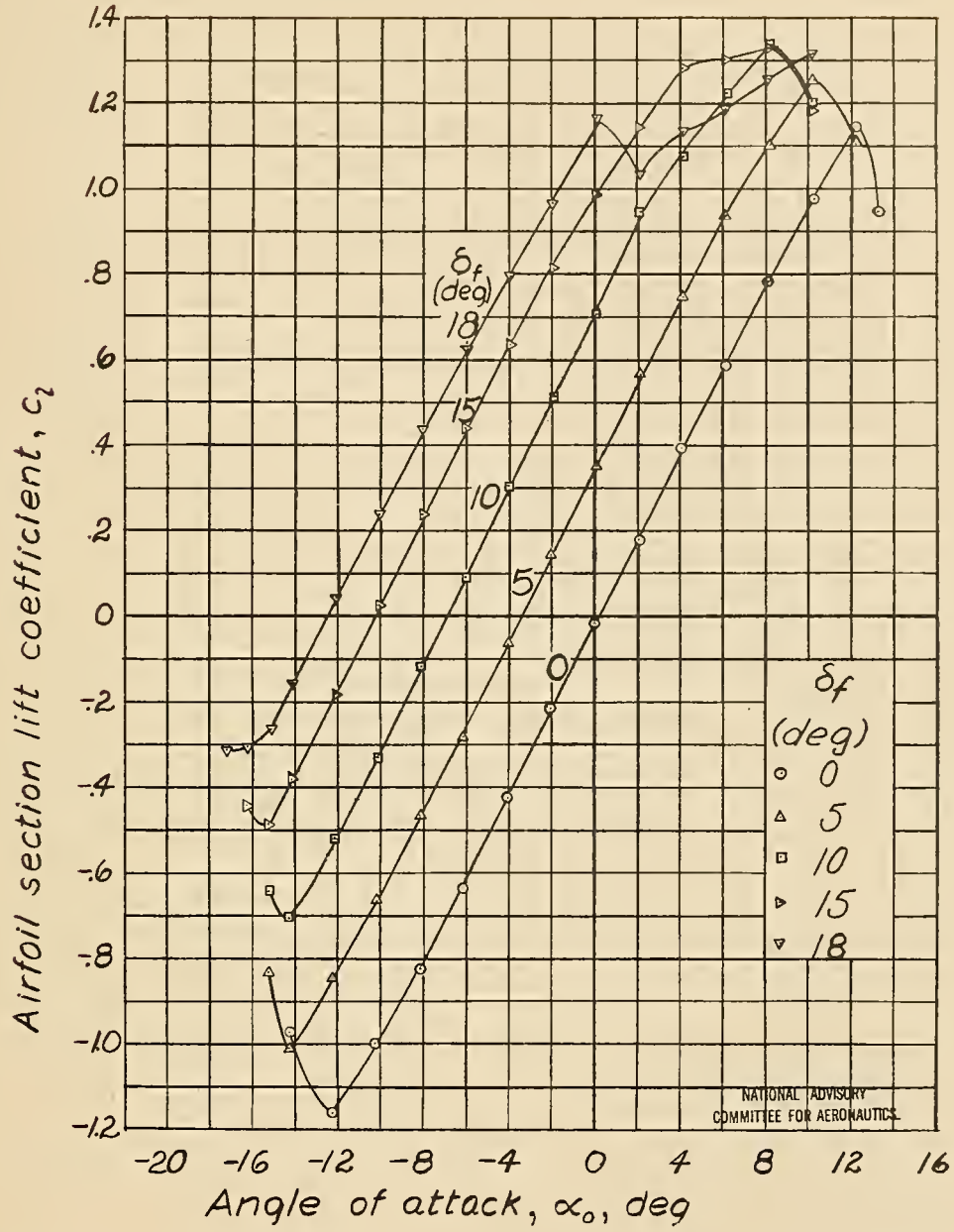

Figure 9.-Aerodynamic section characteristics of an NACA 0009 airfoil with a 0.40c flap having a 0.50c_f overhang with blunt nose. Flap gap sealed; tab, 0.20c_f; tab gap, 0.001c; $\delta_t = 0°$.

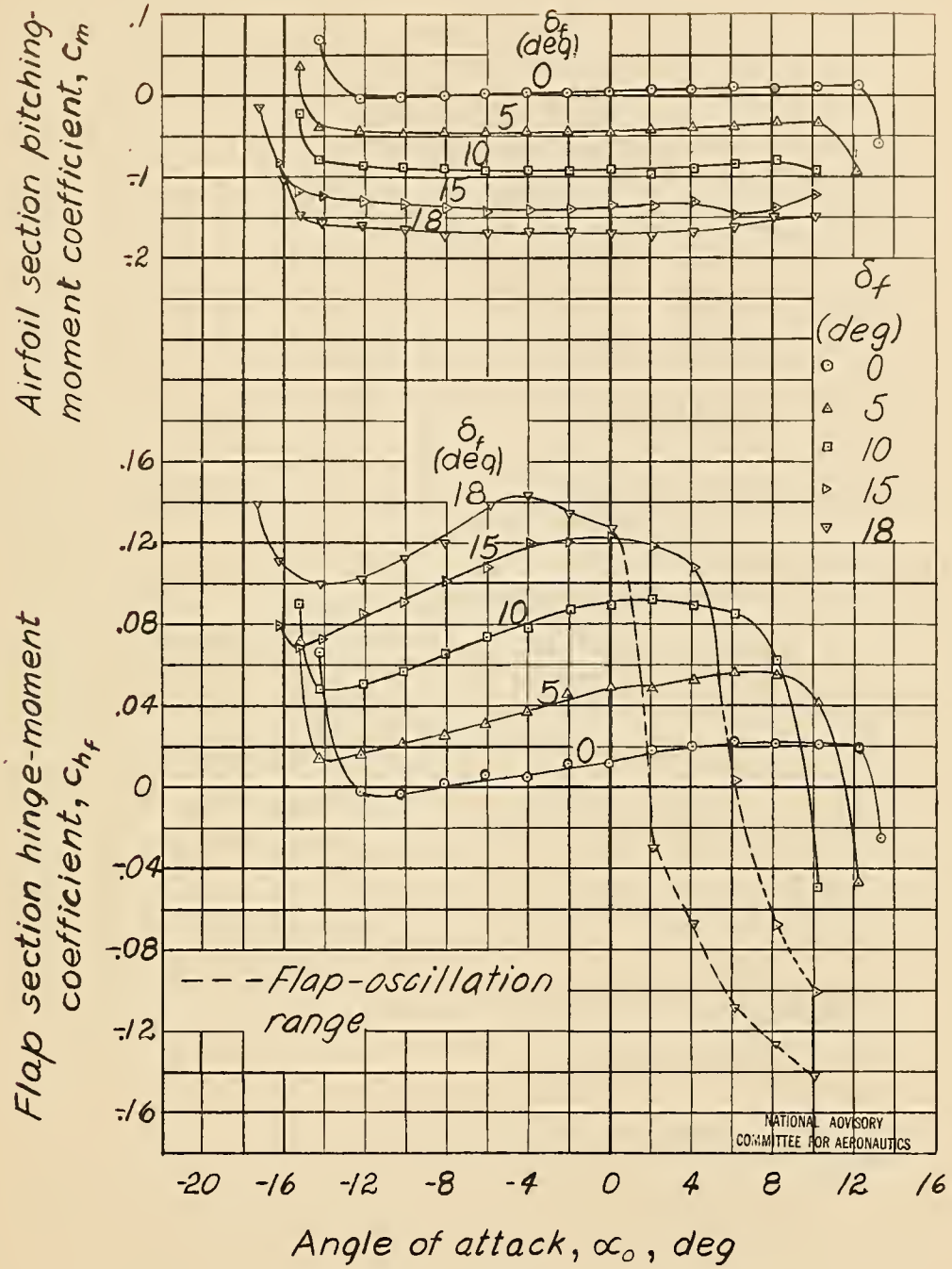

Figure 9.-Concluded.

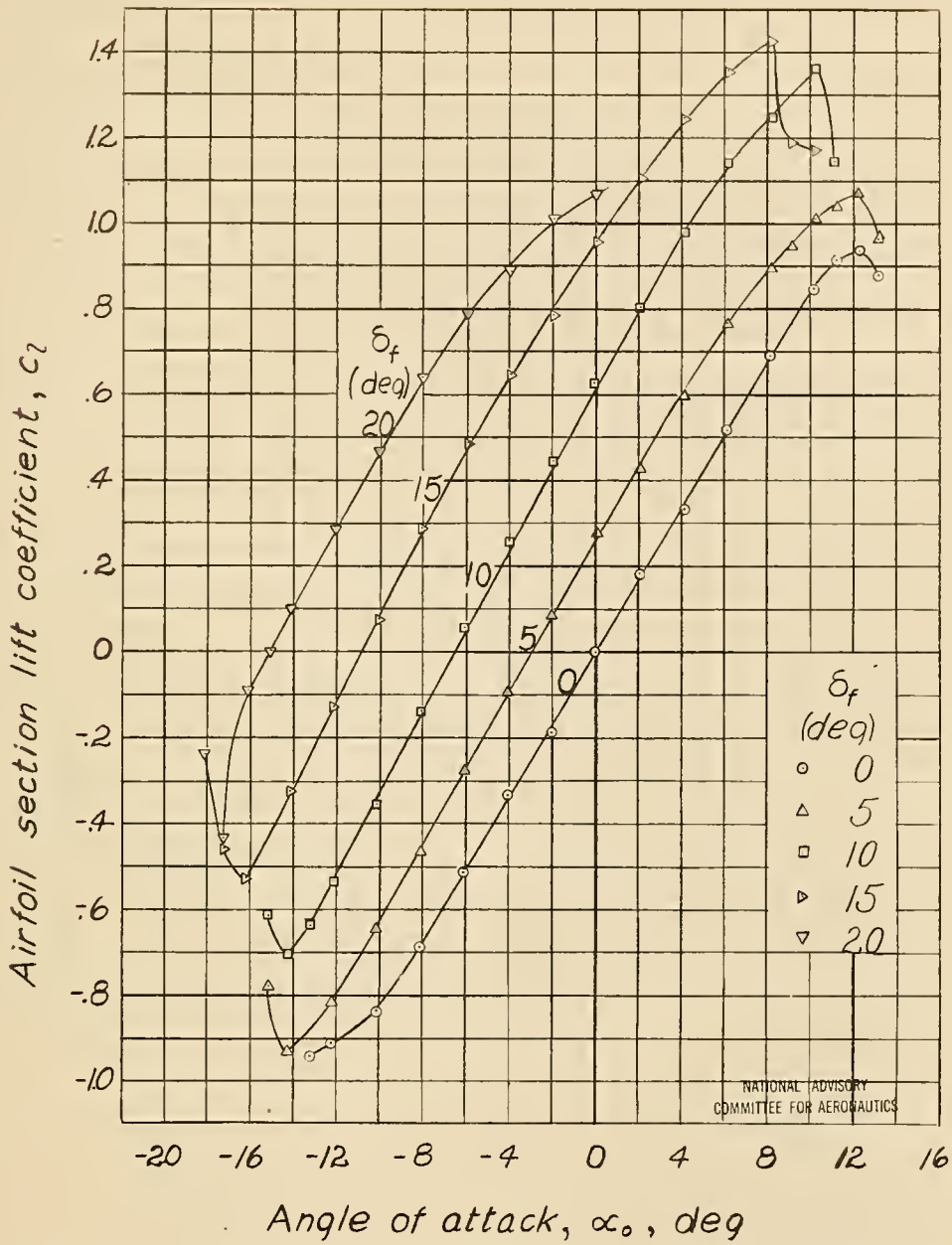

Figure 10.-Aerodynamic section characteristics of an NACA 0009 airfoil with a 0.40c flap having a 0.50c_f overhang with elliptical nose. Flap gap, 0.005c; tab, 0.20c_f; tab gap, 0.001c; $\delta_t = 0°$.

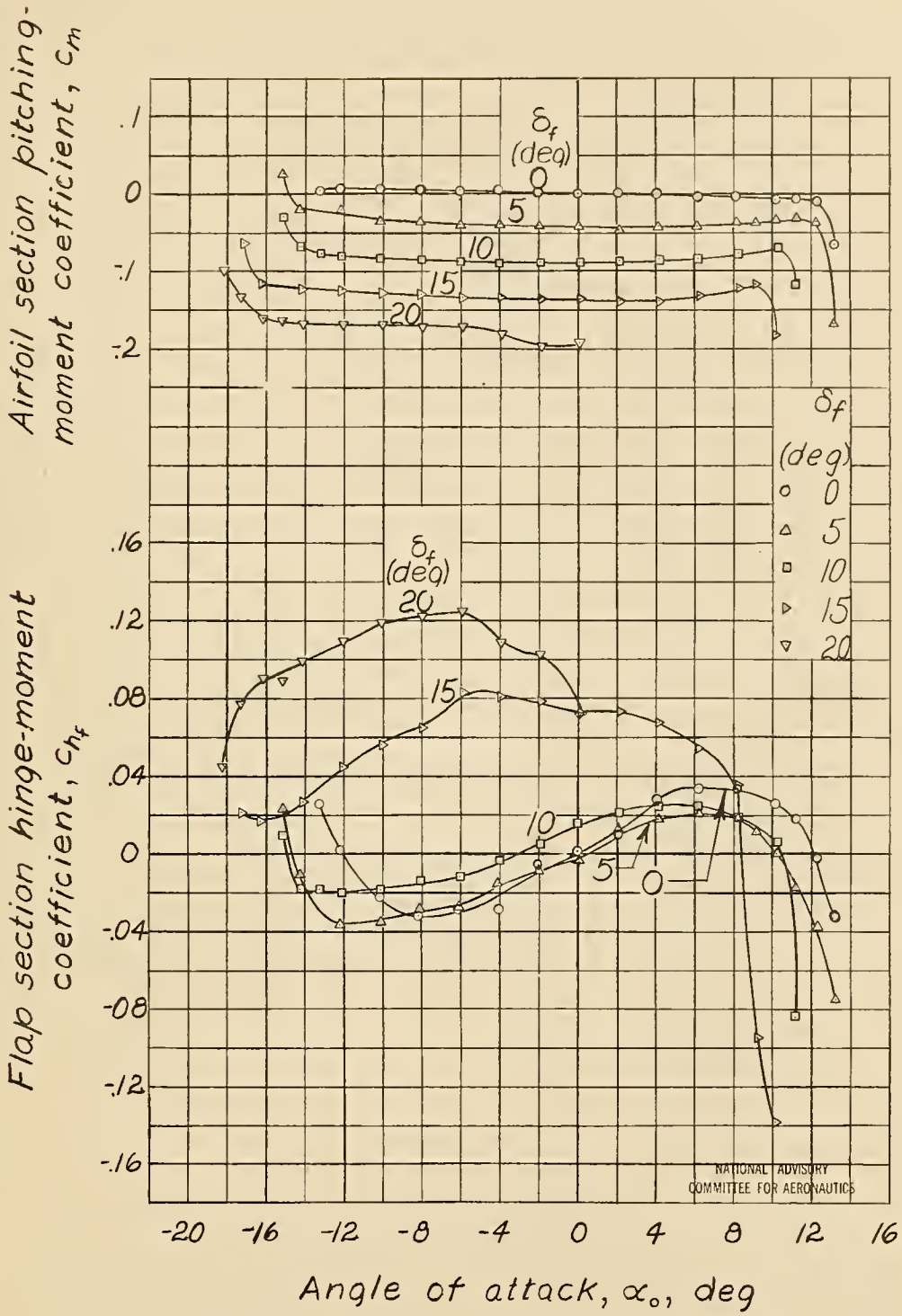

Figure 10.-Concluded.

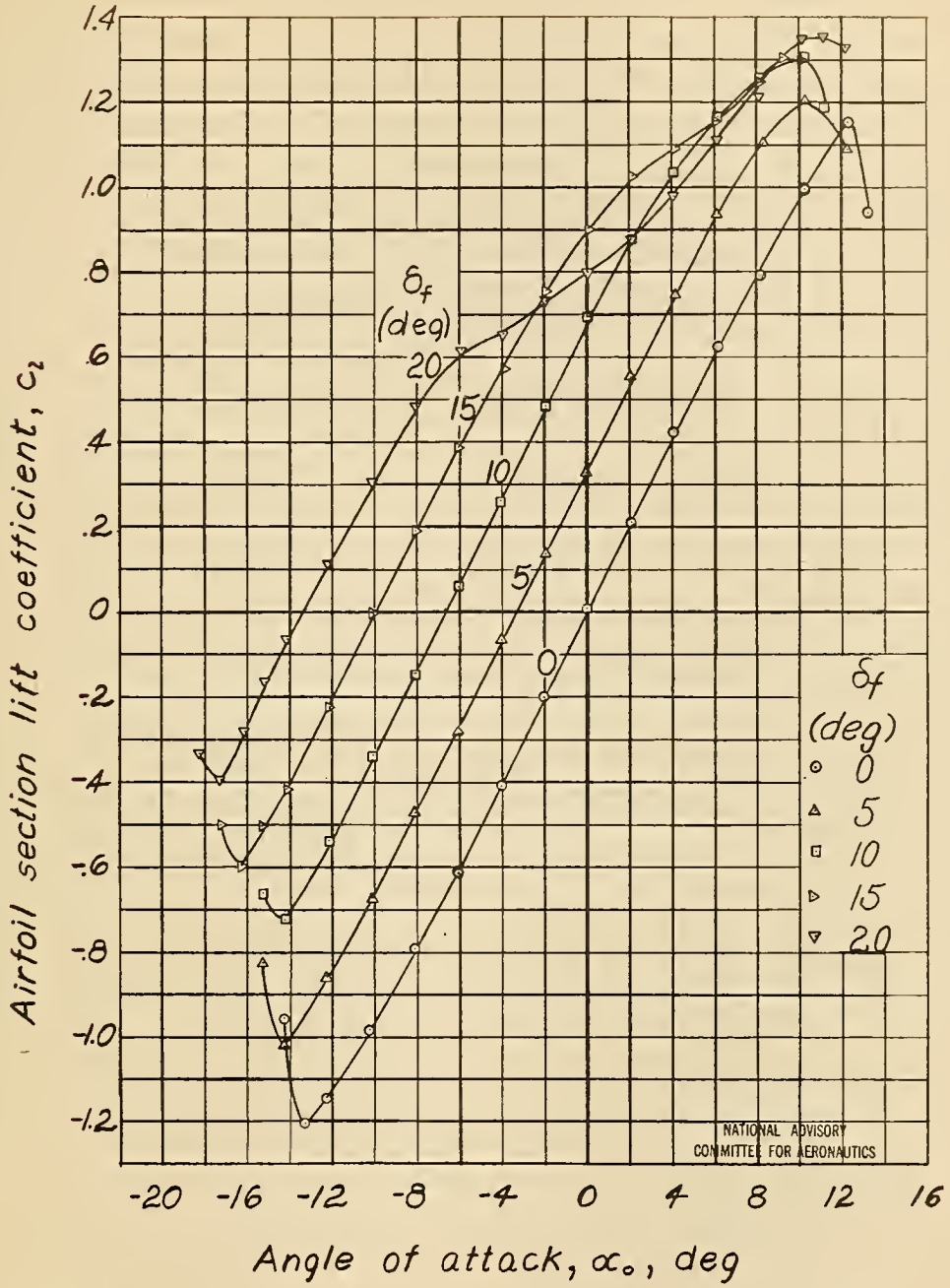

Figure 11.- Aerodynamic section characteristics of an NACA 0009 airfoil with a 0.40c flap having a 0.50c_f overhang with elliptical nose. Flap gap sealed; tab, 0.20c_f ; tab gap, 0.001c ; δ_t=0

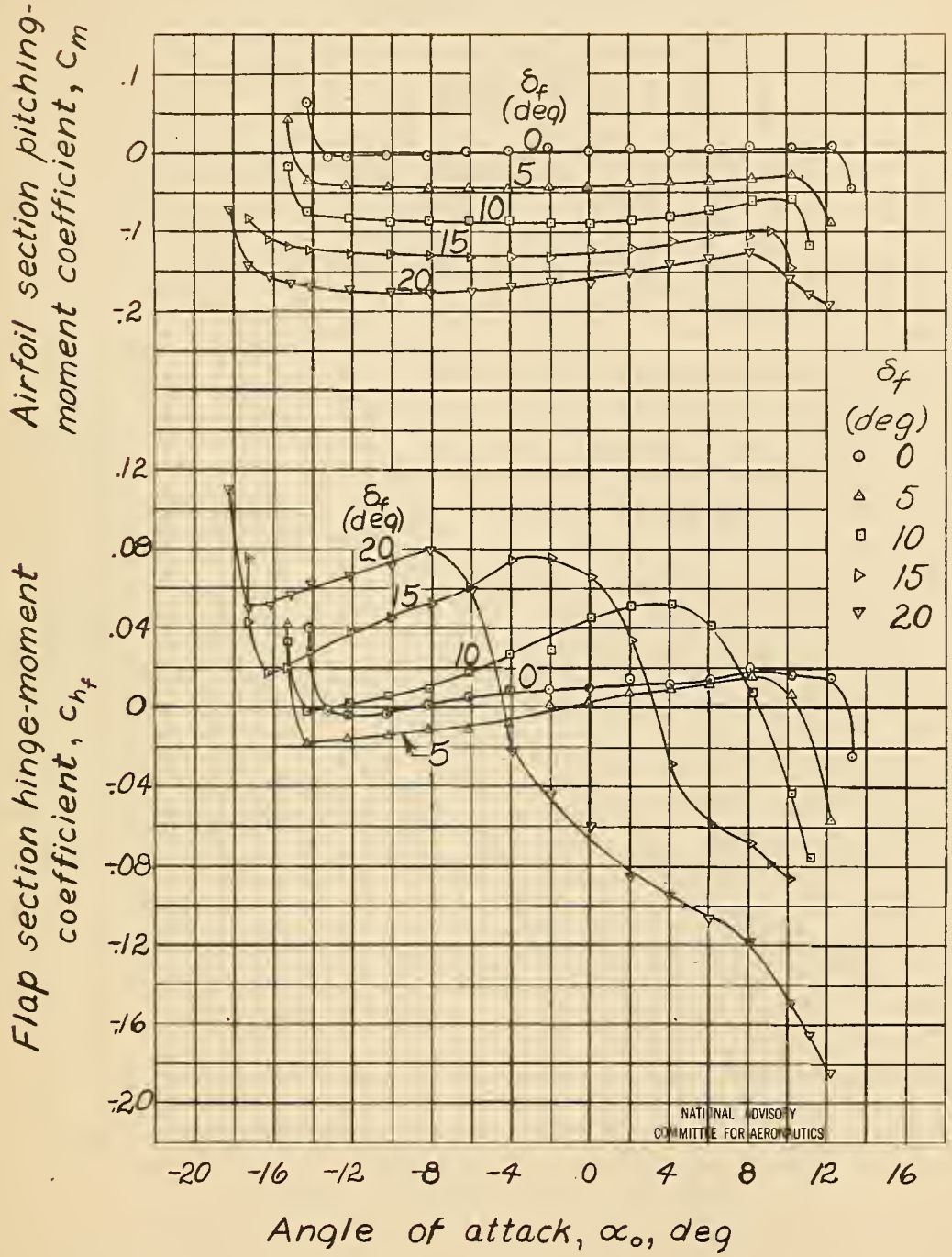

Figure 11.-Concluded.

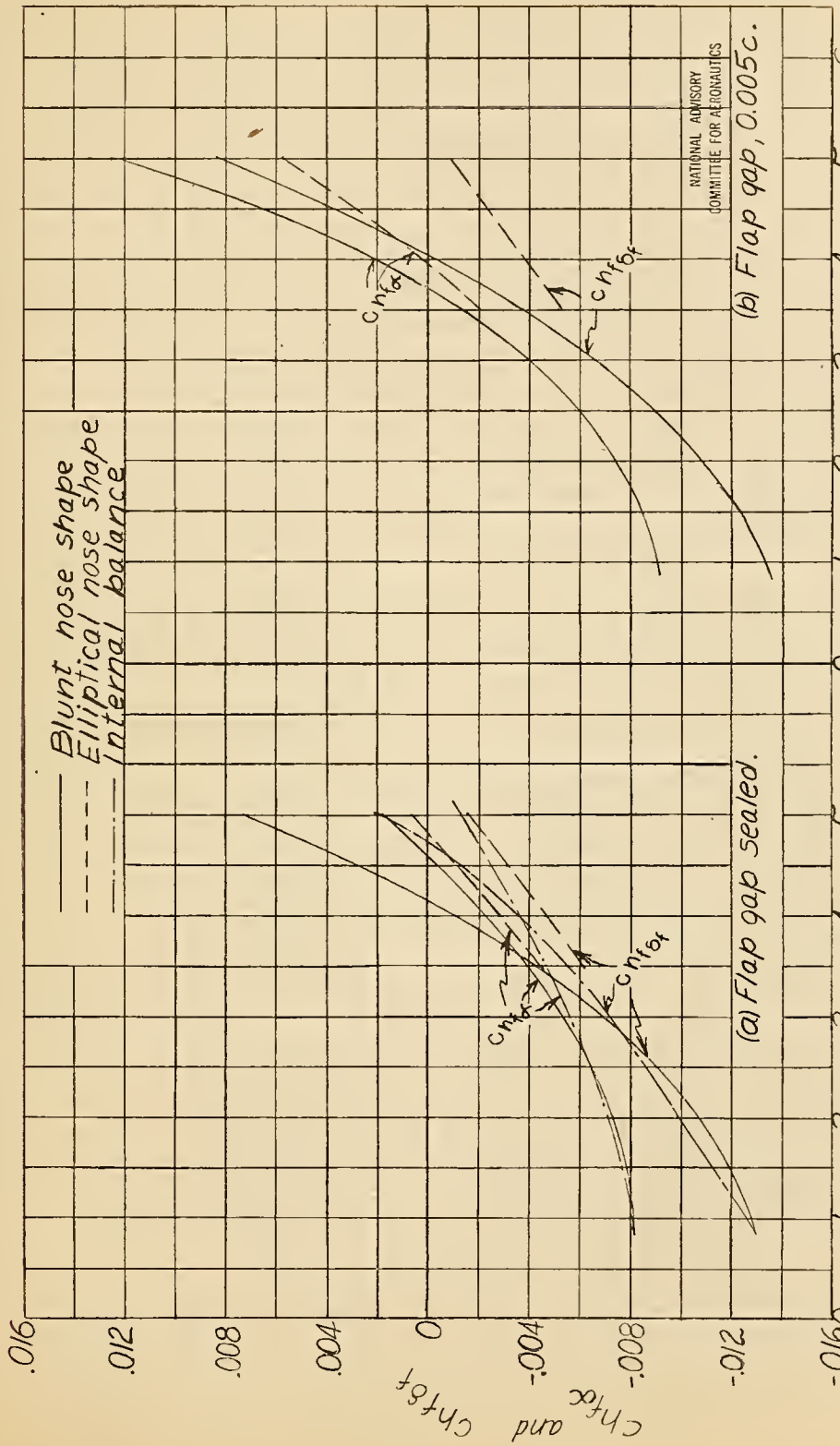

Figure 12.- Variation of flap section hinge-moment parameters with overhang on an NACA 0009 airfoil with a 0.40c flap. Tab $0.20c_f$; tab gap, 0.001c; $\delta_t = 0°$.

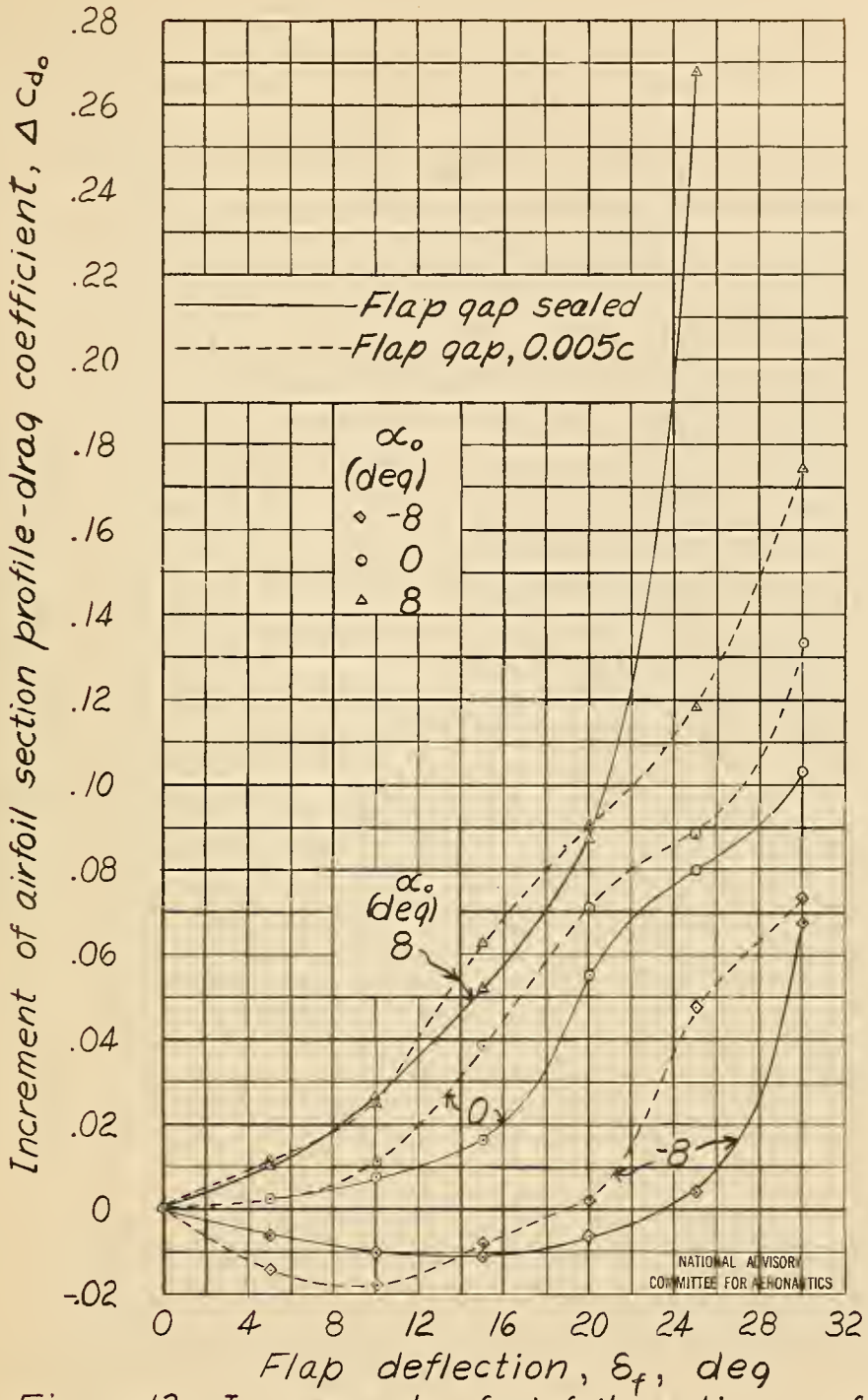

Figure 13.– Increment of airfoil section profile-drag coefficient caused by deflection of a 0.40c plain flap with flap gap sealed and with flap gap, 0.005c. Tab, 0.20 c_f; tab gap, 0.001c; $\delta_t = 0°$.

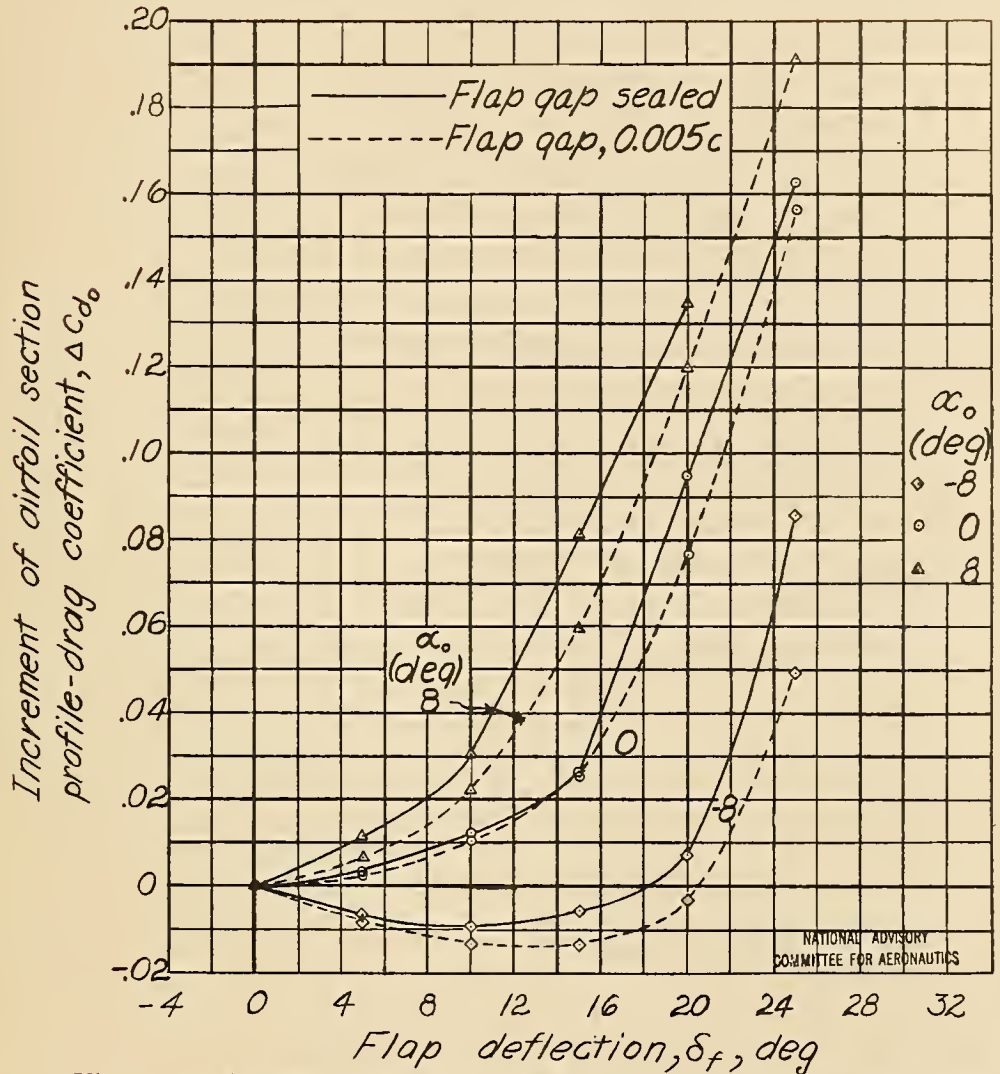

Figure 14.- Increment of airfoil section profile-drag coefficient caused by deflection of 0.40c flap having a 0.35c_f blunt overhang with flap gap sealed and with flap gap, 0.005c. Tab, 0.20 c_f; tab gap, 0.001c; $\delta_t = 0°$.

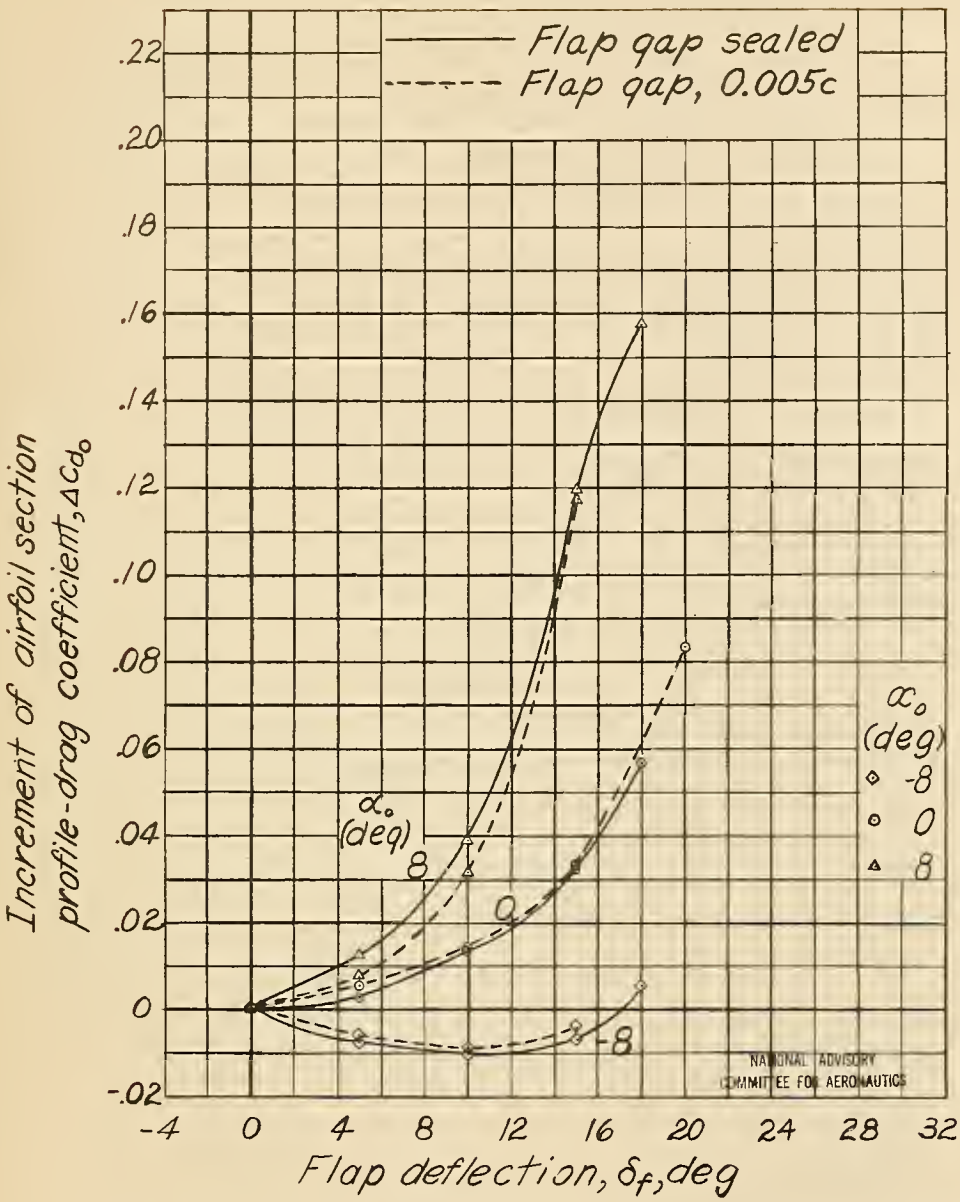

Figure 15.-Increment of airfoil section profile-drag coefficient caused by deflection of 0.40c flap having a 0.50c_f blunt overhang with flap gap sealed and with flap gap 0.005c. Tab, 0.20 c_f; tab gap, 0.001c; $\delta_t = 0°$.

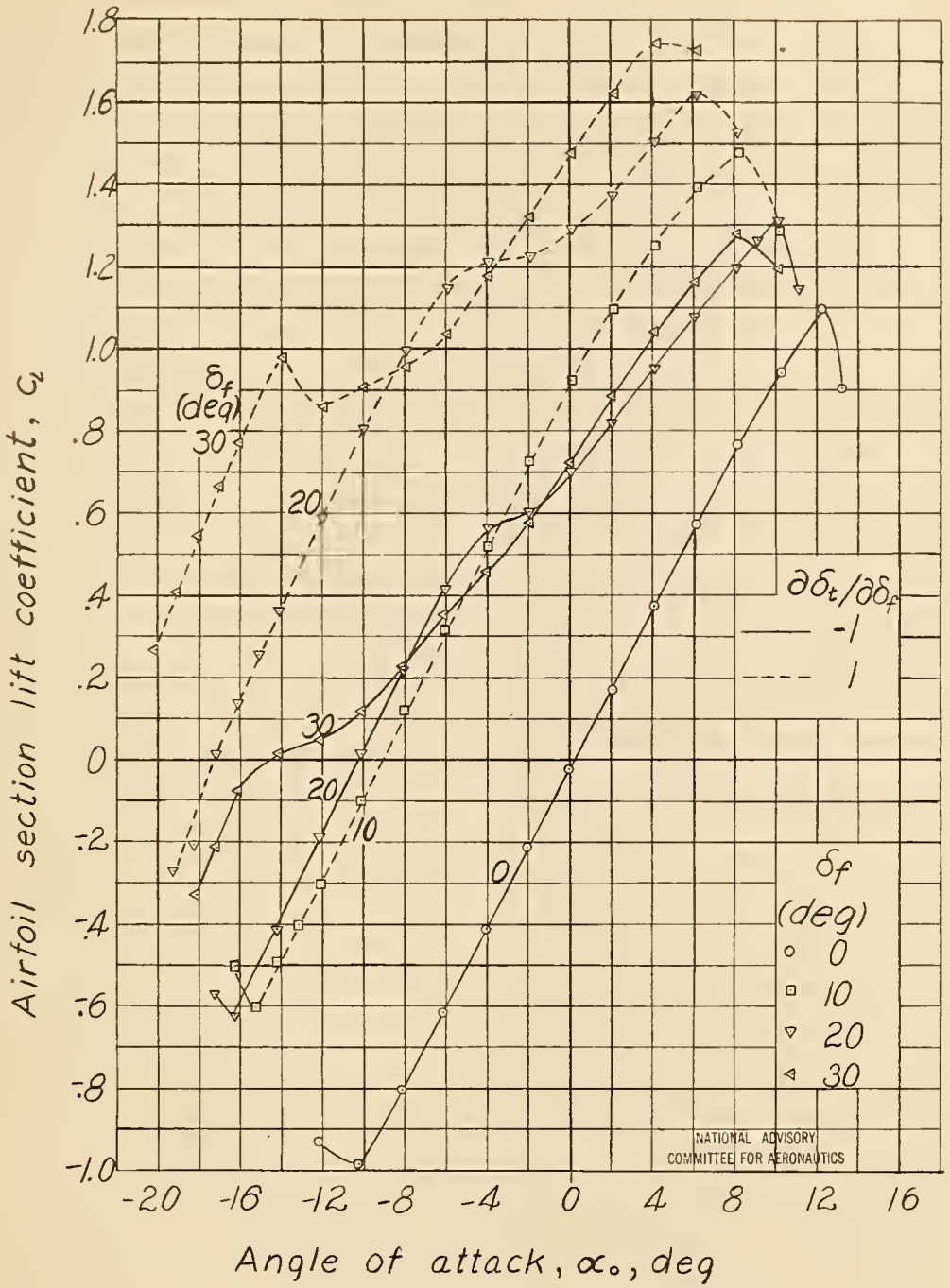

Figure 16.-Aerodynamic section characteristics of an NACA 0009 airfoil with a 0.40c plain flap having a 0.20c_f plain tab with $\frac{\partial\delta_t}{\partial\delta_f}$ = -1, 1. Flap gap sealed; tab gap, 0.001c.

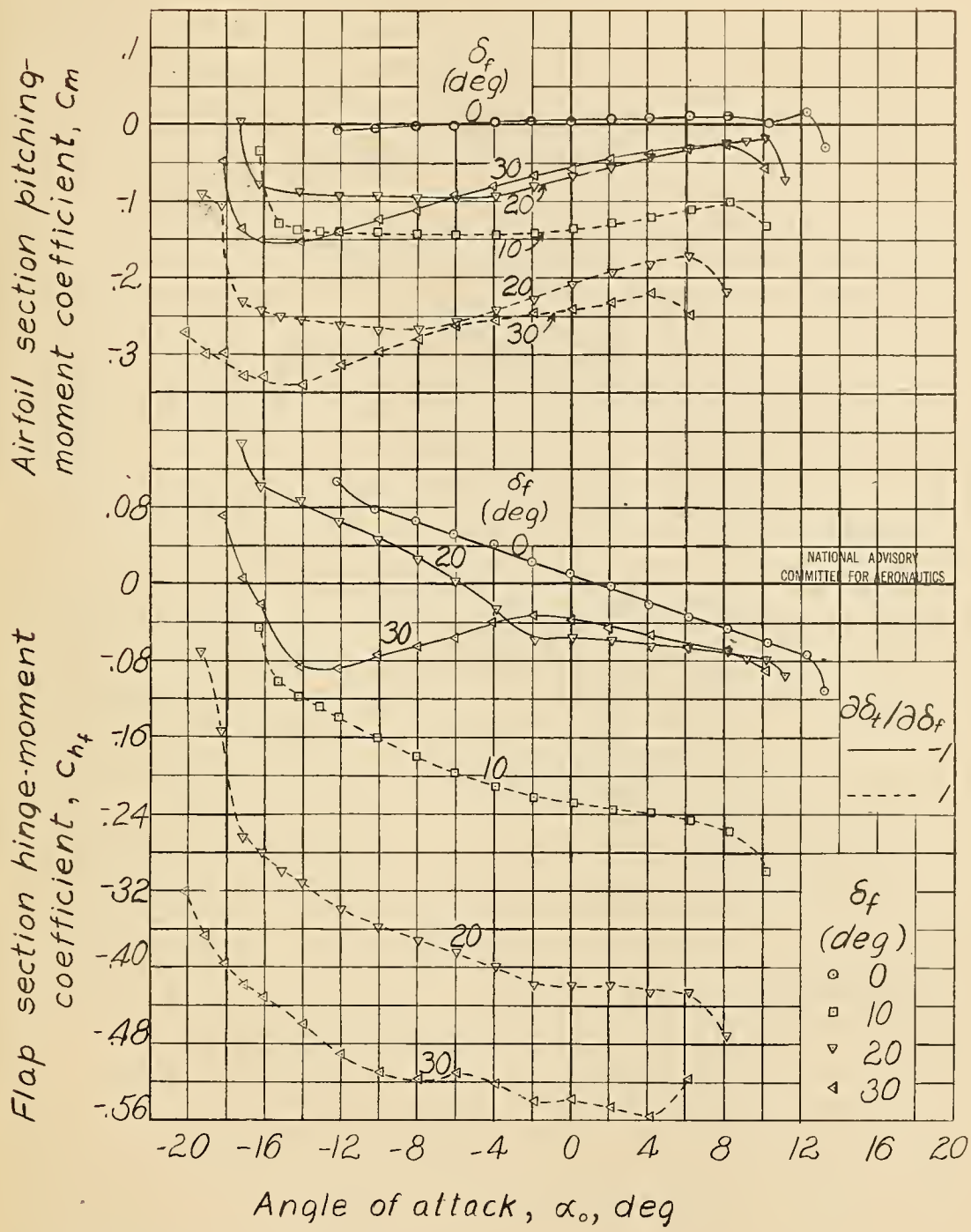

Figure 16.- Continued.

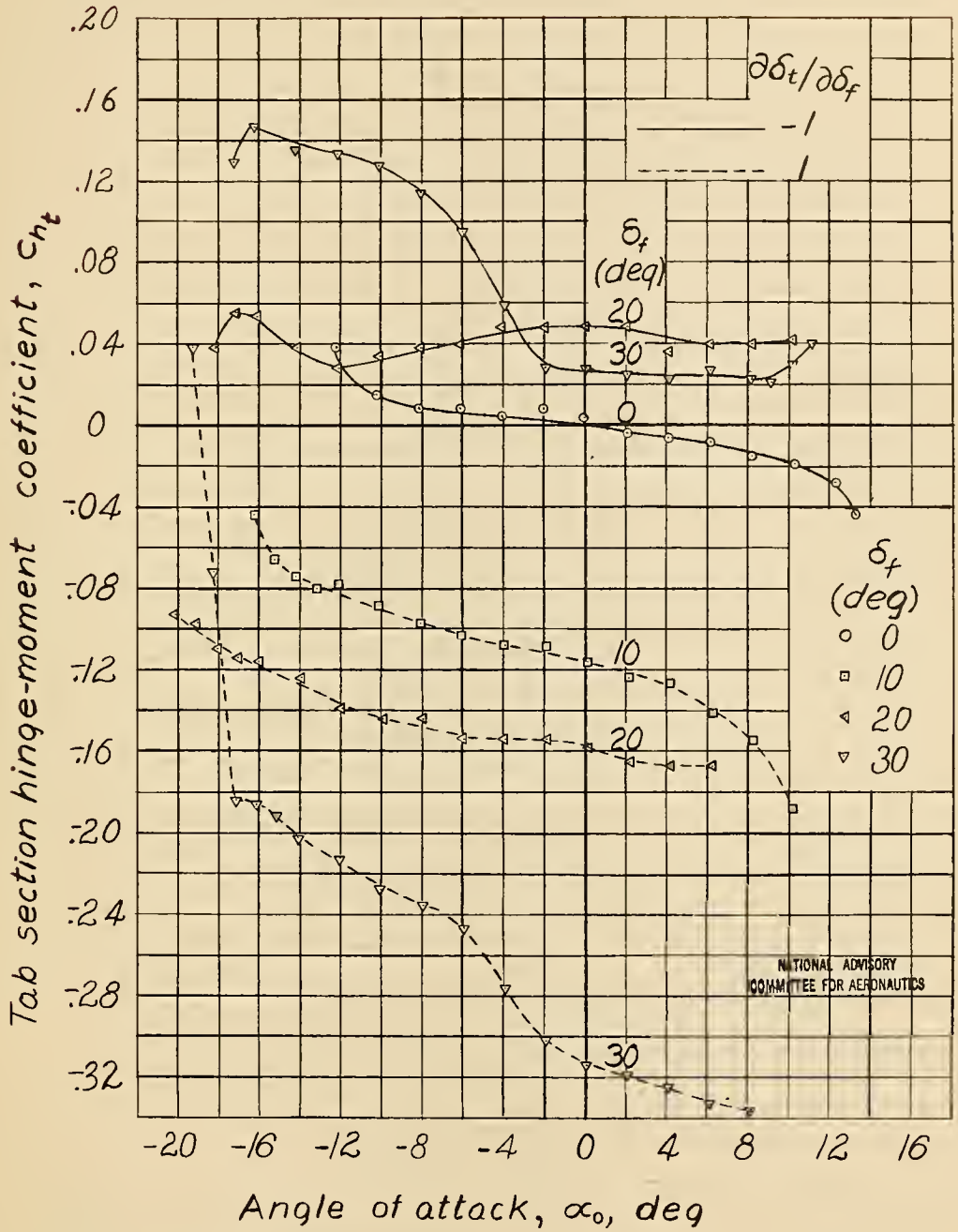

Figure 16.-Concluded.

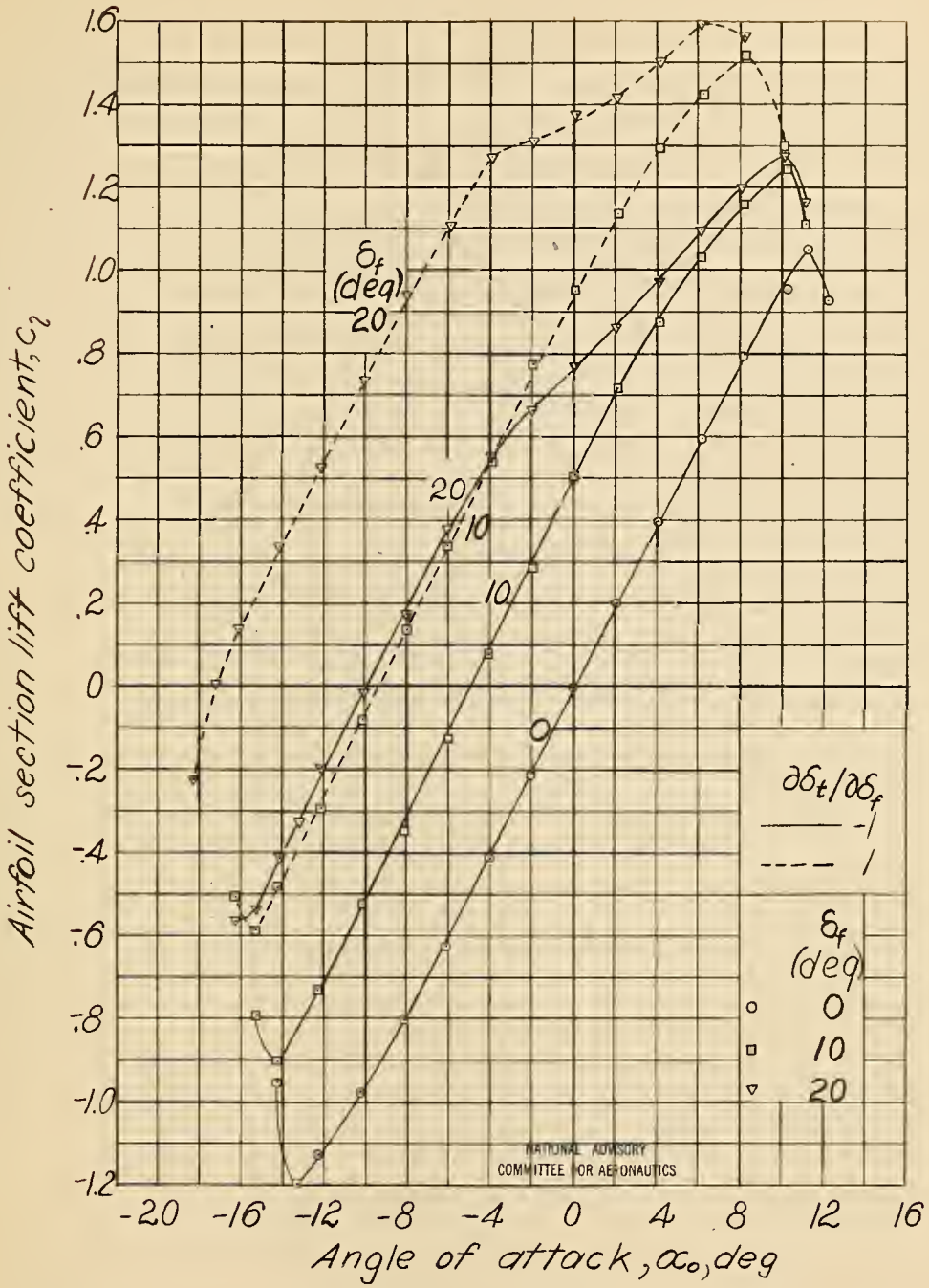

Figure 17.- Aerodynamic section characteristics of an NACA 0009 airfoil with a 0.40c flap having a 0.35c_f overhang with elliptical nose and having a plain tab with $\frac{\partial\delta_t}{\partial\delta_f}$ =-1, 1. Flap gap sealed; tab gap, 0.001c.

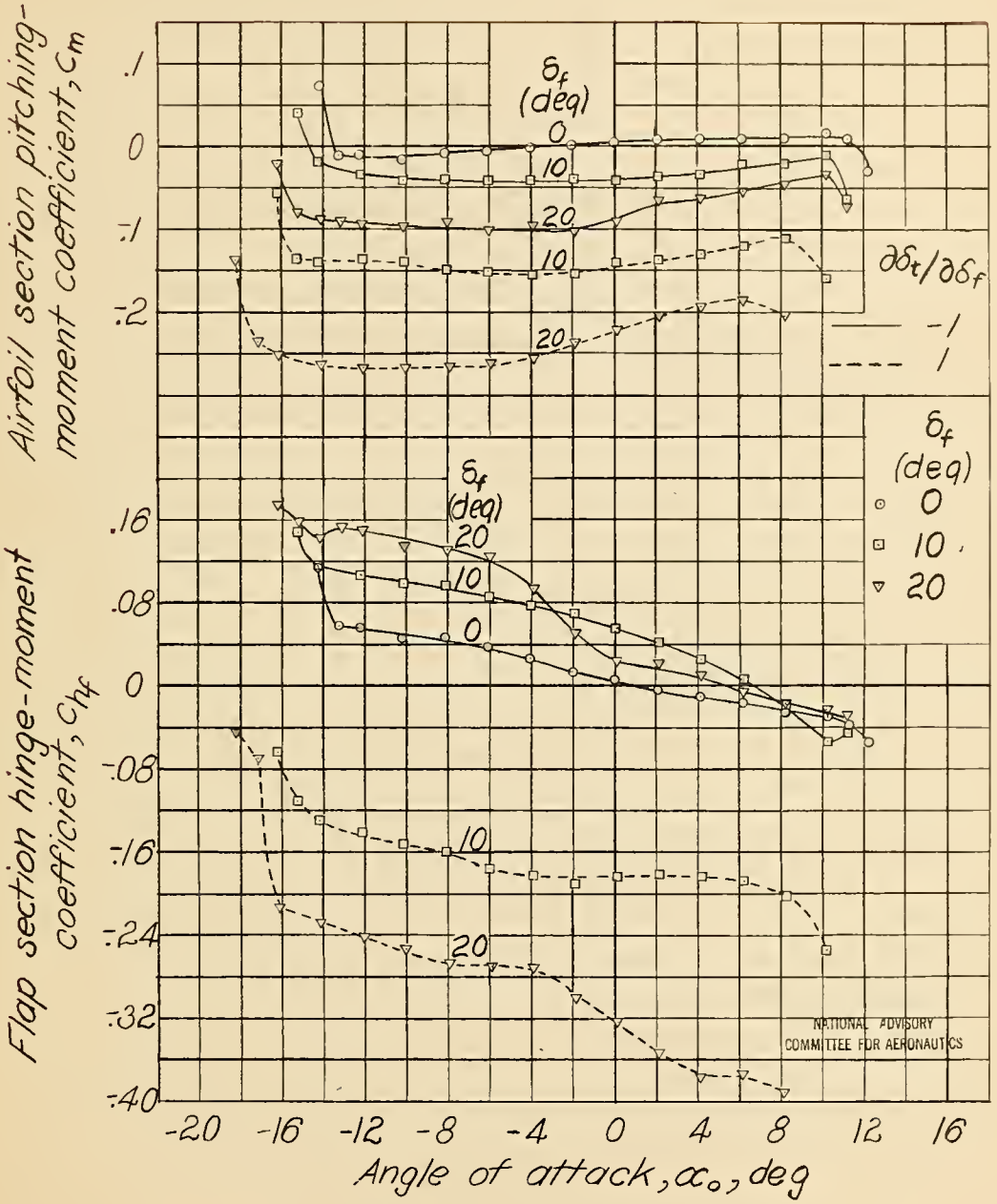

Figure 17.- Continued.

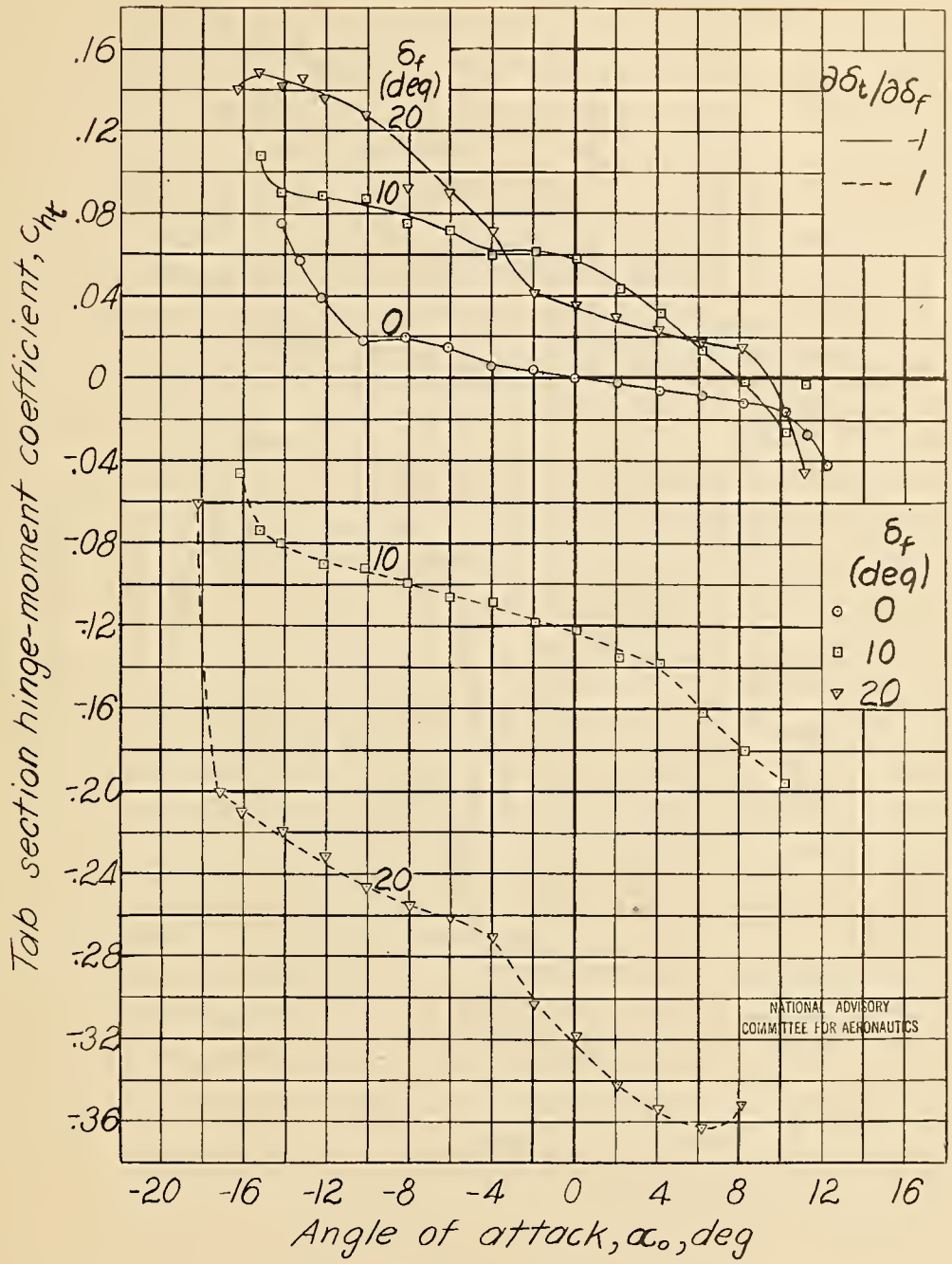

Figure 17.- Concluded.

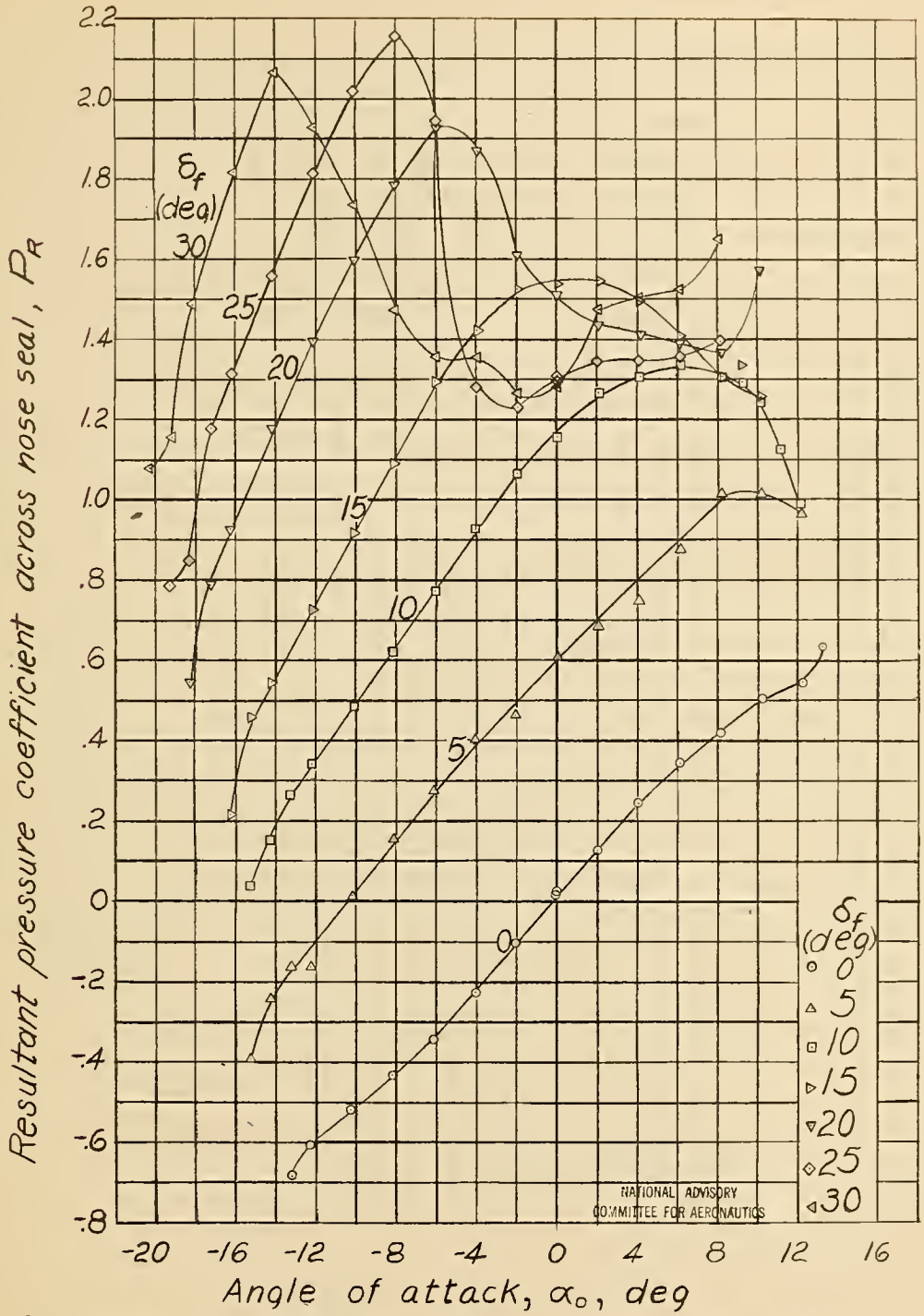

Figure 18.- Variation with angle of attack of resultant pressure coefficient across the nose seal of a 0.40c plain flap on an NACA 0009 airfoil. Tab, 0.20 c_f; tab gap, 0.001c; $\delta_t = 0°$

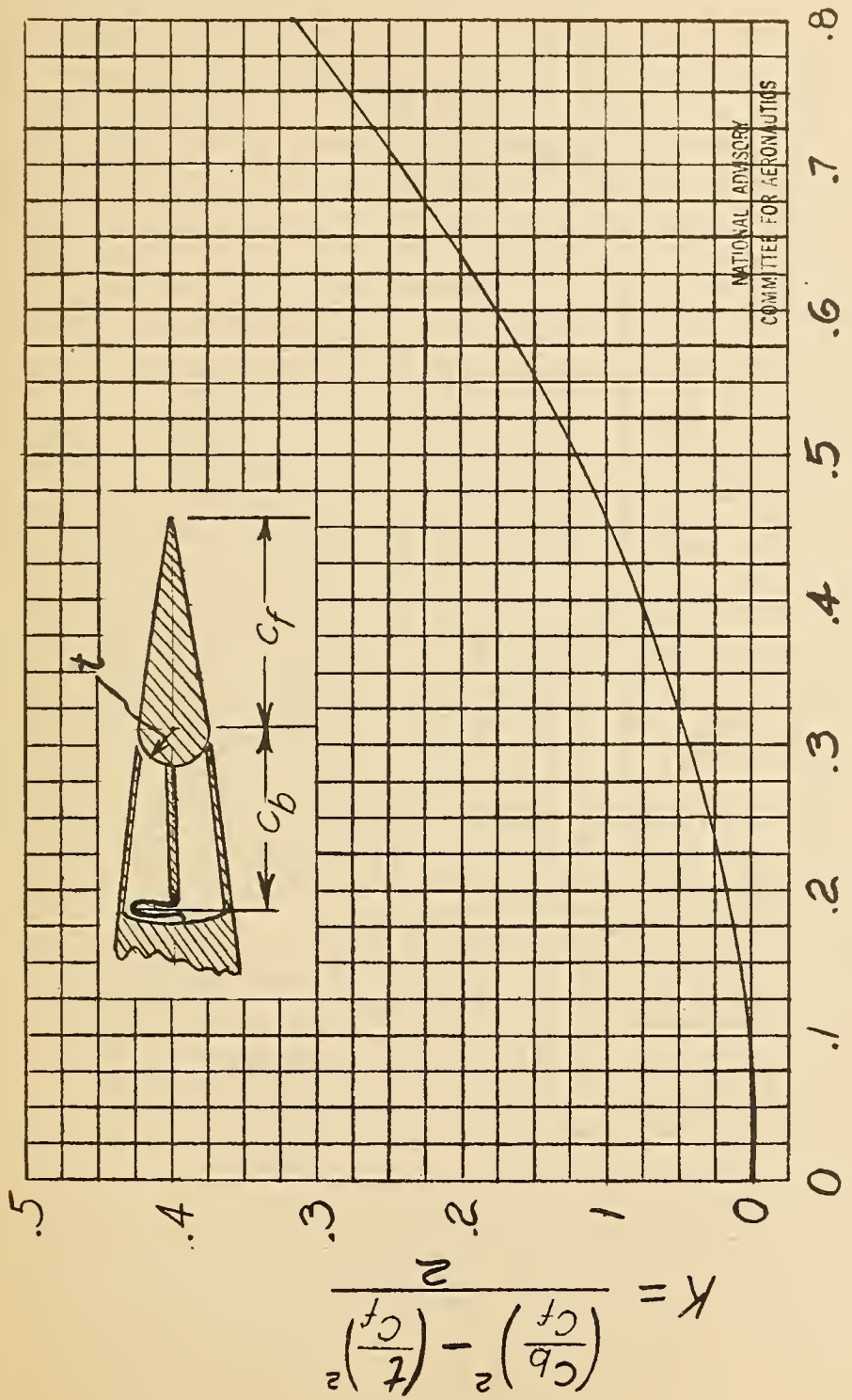

Figure 19. - Variation with internal-balance length of the constant K used in determining the section hinge-moment coefficients of a plain 0.40c flap fitted with an internal balance.

UNIVERSITY OF FLORIDA
3 1262 08106 553 3

UNIVERSITY OF FLORIDA
DOCUMENTS DEPARTMENT
120 MARSTON SCIENCE LIBRARY
P.O. BOX 117011
GAINESVILLE, FL 32611-7011 USA